

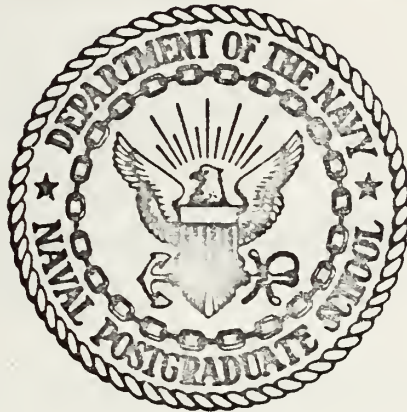
THE MODELLING OF MONSOON CIRCULATION
DURING NORTHERN SUMMER

James Richard Bellis

DUDLEY KNOX LIBRARY
NAVAL POSTGRADUATE SCHOOL
MONTEREY, CALIFORNIA 93940

NAVAL POSTGRADUATE SCHOOL

Monterey, California



THESIS

THE MODELLING OF MONSOON CIRCULATION

DURING NORTHERN SUMMER

by

James Richard Bellis

September 1975

Thesis Advisor:

C.-P. Chang

T169641

Approved for public release; distribution unlimited.

REPORT DOCUMENTATION PAGE		READ INSTRUCTIONS BEFORE COMPLETING FORM
1. REPORT NUMBER	2. GOVT ACCESSION NO.	3. RECIPIENT'S CATALOG NUMBER
4. TITLE (and Subtitle) The Modelling of Monsoon Circulation During Northern Summer		5. TYPE OF REPORT & PERIOD COVERED Master's Thesis September 1975
7. AUTHOR(s) James Richard Bellis		6. PERFORMING ORG. REPORT NUMBER
9. PERFORMING ORGANIZATION NAME AND ADDRESS Naval Postgraduate School Monterey, California 93940		8. CONTRACT OR GRANT NUMBER(s)
11. CONTROLLING OFFICE NAME AND ADDRESS Naval Postgraduate School Monterey, California 93940		10. PROGRAM ELEMENT, PROJECT, TASK AREA & WORK UNIT NUMBERS
14. MONITORING AGENCY NAME & ADDRESS (if different from Controlling Office) Naval Postgraduate School Monterey, California 93940		12. REPORT DATE September 1975
		13. NUMBER OF PAGES 55
		15. SECURITY CLASS. (of this report) Unclassified
		15a. DECLASSIFICATION/DOWNGRADING SCHEDULE
16. DISTRIBUTION STATEMENT (of this Report) Approved for public release; distribution unlimited.		
17. DISTRIBUTION STATEMENT (of the abstract entered in Block 20, if different from Report)		
18. SUPPLEMENTARY NOTES		
19. KEY WORDS (Continue on reverse side if necessary and identify by block number)		
20. ABSTRACT (Continue on reverse side if necessary and identify by block number) The numerical model formulated by Monaco and Williams (1975), which is essentially similar to the UCLA general circulation model, was used to simulate the northern summer monsoon. The model was truncated to a three-level window model which covers the region, 0° - 180°E and 18°S - 46°N only. The zonally asymmetric motions are driven by a specified heating function which resembles the 200 mb seasonal mean divergence field observed by Krishnamurti and Rogers (1970). Major planetary-scale		

features of the monsoon are reasonably simulated along with development of synoptic scale transient disturbances at upper levels. The results indicate that the present model is suitable for more elaborate studies of the southwest monsoon.

The Modelling of Monsoon Circulation
During Northern Summer

by

James Richard Bellis
Lieutenant Commander, United States Navy
B.S., Colorado College, 1962

Submitted in partial fulfillment of the
requirements for the degree of

MASTER OF SCIENCE IN METEOROLOGY

from the
NAVAL POSTGRADUATE SCHOOL
September 1975

Thesis

§ 20528

c. 1

ABSTRACT

The numerical model formulated by Monaco and Williams (1975), which is essentially similar to the UCLA general circulation model, was used to simulate the northern summer monsoon. The model was truncated to a three-level window model which covers the region, 0° - 180° E and 18° S - 46° N only. The zonally asymmetric motions are driven by a specified heating function which resembles the 200 mb seasonal mean divergence field observed by Krishnamurti and Rogers (1970). Major planetary-scale features of the monsoon are reasonably simulated along with development of synoptic scale transient disturbances at upper levels. The results indicate that the present model is suitable for more elaborate studies of the southwest monsoon.

TABLE OF CONTENTS

I. INTRODUCTION - - - - - 9

II. DESCRIPTION OF THE NUMERICAL MODEL - - - - - 14

 A. BASIC MODEL- - - - - 14

 B. THE GRID SYSTEM- - - - - 14

 C. DIABATIC HEATING AND DAMPING - - - - - 15

 D. INTEGRATION SCHEME AND INITIAL CONDITIONS- - - - - 16

III. RESULTS- - - - - 18

 A. TIME MEAN FIELD- - - - - 18

 B. TRANSIENT FIELD- - - - - 21

IV. CONCLUSIONS- - - - - 23

LIST OF REFERENCES - - - - - 53

INITIAL DISTRIBUTION LIST- - - - - 54

LIST OF FIGURES

1.	Horizontal distribution of variables - - - - -	24
2.	Vertical index - - - - -	25
3.	Horizontal distribution of heating - - - - -	26
4.	a. 250 mb time-mean wind field- - - - -	27
	b. 500 mb time-mean wind field- - - - -	28
	c. 850 mb time-mean wind field- - - - -	29
5.	a. 250 mb time-mean geopotential field- - - - -	30
	b. 500 mb time-mean geopotential field- - - - -	31
	c. 850 mb time-mean geopotential field- - - - -	32
6.	a. 250 mb time-mean temperature field - - - - -	33
	b. 500 mb time-mean temperature field - - - - -	34
	c. 850 mb time-mean temperature field - - - - -	35
7.	400 mb time-mean vertical velocity - - - - -	36
8.	a. 250 mb time-mean divergence field- - - - -	37
	b. 500 mb time-mean divergence field- - - - -	38
	c. 850 mb time-mean divergence field- - - - -	39
9.	a. 250 mb time-mean vorticity field - - - - -	40
	b. 500 mb time-mean vorticity field - - - - -	41
	c. 850 mb time-mean vorticity field - - - - -	42
10.	a. Time-longitude vorticity section at 12°N and time series of longitudinally mean zonal winds - - -	43
	b. Time-longitude divergence section at 12°N- - - - -	44

11.	a.	Time-longitude vorticity section at 24°N and time series of longitudinally mean zonal winds - - - - -	45
	b.	Time-longitude divergence section at 24°N- - - - -	46
12.	a.	250 mb wind field at day 25- - - - -	47
	b.	250 mb wind field at day 26- - - - -	48
	c.	250 mb wind field at day 27- - - - -	49
	d.	250 mb wind field at day 28- - - - -	50
	e.	250 mb wind field at day 29- - - - -	51
	f.	250 mb wind field at day 30- - - - -	52

ACKNOWLEDGEMENTS

The author wishes to express his thanks to Dr. R. T. Williams and Dr. C. P. Chang for their guidance in this thesis. Mr. J. ZuVer of FNWC, Mr. S. Rinard, and Mr. R. Schwanz of NPS contributed heavily towards the data handling. All calculations were carried out at the W. R. Church Computer Center.

I. INTRODUCTION

For several centuries scientists have conjectured about the circulation patterns evidenced in the tropical and subtropical areas. As early as 1686 Halley suggested that the monsoon circulation was driven by differential heating of land and water masses. In 1887 Dallas was quoted when speaking of the Indian monsoon, "...the condensation of vapors and consequent release of latent heat suffice to prolong the existence of the indraught toward India." When speaking of monsoon many people may relate it to the aforementioned pressure differential and associated wind changes. Indeed this may have been the original concept of using this word. Derived from the Arab word for season, mausin, monsoon was used first in context to refer to the winds over the Arabian Sea blowing six months from the northeast and six months from the southwest. However, for others it may be used to describe the occurrence of heavy seasonal rainfall as is the case in India. The reversal of wind directions and the onset or end of the rainy seasons may or may not coincide depending on the geographic location, but a general relationship does exist. For the purpose of this paper the word monsoon will be used to describe the general seasonal circulation over the tropics and subtropics including its associated wind, pressure, temperature and precipitation fields. Our discussion will be limited to the northern summer only.

Recently many meteorologists have revived the interest of studying the monsoon circulation. The general region influenced by the monsoon

encompasses a large portion of the earth's surface, but available data are far from abundant due to the limited observation network in this area. However, principal circulation features of the Northern Hemisphere during summer are quite well known. They may be described by the following time-mean systems in the upper troposphere: (1) the Tibetan high, (2) African high, (3) Mexican high, (4) mid-Atlantic trough, (5) mid-Pacific trough, and (6) the Indian easterly jet. These upper systems represent a vigorous east-west overturning on a planetary scale. The intensity of this overturning was found by Krishnamurti (1971) to be at least comparable to that of the more familiar Hadley cell during one northern summer.

The reversal of flow pattern between seasons is most intense and persistent over India and southeast Asia. These regions plus the Tibetan Highland in southwestern China may be viewed as the most active areas for the summer monsoon. The Tibetan high is a warm high whose formation is thought to be related by the thermal and mechanical effects of the Tibetan Plateau. It is known that latent heat release due to shallow and deep cumulus convection must play an important role in the maintenance of the upper anticyclone. This high pressure system capping a surface low also acts as a block to the mean zonal wind. The upper easterly jet is situated mainly at the southern edge of the anticyclone.

In contrast to the divergent outflow of the Tibetan high the tropical upper tropospheric troughs (TUTT) in the Pacific and Atlantic Oceans are areas of flow convergence. Here the cold air sinks which together with the rising warm air in the high areas converts potential energy into kinetic energy on a planetary scale. Both troughs are observed to tilt from southwest to northeast. According to the

observation by Krishnamurti (1971), the tilt of the long waves is correlated to the mean easterly flow such that at 200 mb a divergence of momentum flux feeds kinetic energy into the mean zonal flow from the quasi-steady planetary-scale long waves. Imbedded in the zonal and planetary scale flow are the synoptic-scale waves which are observed to be highly transient in nature. They seem to receive at least part of their energy from the longer scales by wave-wave and wave-zonal flow interaction. Whether these short waves gain or lose eddy kinetic energy from/to eddy potential energy is not well known at this time. In this study these synoptic-scale disturbances are considered as another important part of the monsoon circulation.

The above observations have stimulated a considerable amount of theoretical and numerical studies of the monsoon circulation. The models have ranged from the very complex general circulation model (GCM) to the simplified but physically more tractable models. The ability of the GCM's in simulating the northern summer monsoon has been demonstrated by Manabe (1973) and Hahn and Manabe (1973) using the GFDL/NOAA (Geophysical Fluid Dynamics Laboratory, National Oceanic and Atmospheric Administration) GCM, and by Washington and Daggupaty (1975) using the NCAR (National Center for Atmospheric Research) GCM. Because of the complexity of the physics, especially the parameterized heating of the GCM, their results are not easy to analyze to understand some of the fundamental mechanisms of the monsoon.

Among the simpler models, Holton and Colton (1972) used a linear one-level barotropic vorticity equation with the observed 200-mb seasonal mean divergence as the forcing. They were successful in

simulating the seasonal mean flow pattern but they found that an extraordinarily large friction is needed to damp the vorticity generation. Otherwise the flow field will become too strong and shift westward by nearly one-quarter cycle in phase. A similar problem was encountered by Abott (1973) in a 3-level quasi-geostrophic model and by Colton (1973) in a one-level primitive-barotropic, semi-spectral model. Both of them used specific forcing to drive the planetary-scale flow to study time-independent, non-linear interaction between scales.

This problem of proper simulation of the phase of the planetary-scale features was addressed by Holton and Colton (1972). They proposed that the fluctuating component of the monsoon heating may have a negative correlation with the fluctuating component of the upper level vorticity which will serve as a damping term for the time-mean vorticity budget. Murakami (1973, 1974) has included a fluctuating heating in his semi-spectral model and seems to have no difficulty in the phase problem. However, his results are somewhat unrealistic in that the vertical profile of vertical velocity differs considerably from observations. The phase problem thus appears to remain unsolved.

As mentioned previously, observations have been made with regard to energetics and their transfer between different circulation scales. Both Colton (1973) and Abott (1973) concluded that the "short-term" or "local" barotropic instability due to the forced planetary-scale flow causes synoptic transient disturbances in the TUTT and easterly jet regions to develop and grow, in agreement with observations. These disturbances may be related to the upper-level synoptic systems observed by Sadler (1967) and Krishnamurti and Rogers (1969). It has been noted

that the strength of precipitation and latent heat release in the monsoon region is strongly influenced by synoptic-scale disturbances. Therefore, in addition to the barotropic effects, thermodynamics must also play a role in the interaction between short and long waves.

The results between different models are not easy to compare because of the differences in model aspects. On the other hand, proper simulation of the various features of the monsoon require a GCM, while an understanding of the physics is easier in a simplified model. Thus it may be desirable to compare results of specified heating with results of parameterized heating from two compatible models.

This study is a first step in such an attempt. Its purpose is to use a GCM with specified heating to simulate the northern summer under certain conditions. Some of the dynamics of the circulation may be studied in the future by varying these conditions, and hopefully all forced results can be used to compare with the same GCM using parameterized heating at a later date. Another purpose is to evaluate the performance of the GCM as formulated by Monaco and Williams (1975), which is essentially similar to the UCLA GCM (Arakawa and Mintz, 1974). This model is currently under consideration for adoption by the Navy as a possible operational model, and its ability to simulate the gross features of monsoon circulation is crucial for tropical prediction.

II. DESCRIPTION OF THE NUMERICAL MODEL

A. BASIC MODEL

The model used is basically similar to that described by Arakawa and Mintz (1974) who used primitive equations in spherical coordinates with "sigma" as the vertical coordinate. The FORTRAN coding was done by Monaco and Williams (1975). In this study the horizontal area is limited to a hemispheric band extending from 18° south to 46°N and 0° to 180°E, with the free-slip conditions used at the latitudinal boundaries and cyclic continuity maintained at the east-west boundaries.

B. THE GRID SYSTEM

The horizontal distribution of variables is illustrated in Figure 1 which is the so-called C-scheme arrangement (Arakawa and Mintz, 1974). The grid spacing is 4 degrees in latitude and longitude. In the vertical seven equally spaced sigma levels are used with three main reporting levels as shown in Figure 2. The sigma coordinate is defined as

$$\sigma \equiv \frac{p - p_t}{\pi} \quad (2.1)$$

where p is the pressure of the sigma level, p_t is the height of the constant tropopause which is set to 100 mb, and π is the "terrain pressure" defined as

$$\pi \equiv p_s - p_t \quad (2.2)$$

The surface pressure, p_s , is set to 1000 mb initially. It follows from (2.1) that

$$\sigma = 0 \text{ at } p = p_t ,$$

$$\sigma = 1 \text{ at } p = p_s ,$$

which are the vertical boundaries of the model. The boundary condition at $\sigma = 1$ and $\sigma = 0$ are both $\frac{d\sigma}{dt} = 0$.

C. DIABATIC HEATING AND DAMPING

In the evaluation of the global model performed by Monaco (1975) no source or sink was included. In this study the main driving force is the diabatic heating so that a source term is added to the thermodynamic energy equation.

Two components of heating are included.

$$Q = Q_x + Q_t , \tag{2.3}$$

where Q_x , the zonally symmetric heating component is given by a continuous adjustment to a specified equilibrium temperature, T^* , using the following formula,

$$Q_x = -\left[\frac{T - T^*(y,\sigma)}{\tau}\right] . \tag{2.4}$$

Here T is the temperature and τ is a specified adjustment time set to two days in this study. The equilibrium temperature T^* is taken from the observation given by Palmen and Newton (1969) for the July climatology with the sigma reporting levels 1 to 3 assumed to be 250, 550, and 850 mbs, respectively. This component maintains the zonally

mean north-south temperature gradient. The zonally asymmetric component, Q_t , is assumed to be time-independent and is derived from the 200-mb time-mean divergence field observed by Krishnamurti (1967) using the following formula:

$$Q(^{\circ}\text{K day}^{-1}) = \text{divergence (sec}^{-1}) \times 10^6. \quad (2.5)$$

The field is then smoothed at the longitudinal boundaries to provide cyclic continuity and is modified at the latitudinal boundaries of the model by reducing the strength of heating by 50% at the points just inside the boundaries and by 90% at boundary points. Fig. 3 shows the horizontal distribution of heating. In the vertical, the full value of heating derived by (2.5) is specified at level 2 and a vertical distribution is assumed such that the heating at level 1 and 3 are 50% and 25%, respectively, of the value at level 2. This vertical distribution is in accord with the observed profile of large-scale heating due to condensation in the tropical Pacific cloud cluster areas. The maximum magnitude of both heating and cooling is $4^{\circ}\text{K day}^{-1}$ at level 2.

Linear damping terms are included in the momentum equation to include the effect of friction. The drag coefficients are $.3 \times 10^{-6} \text{ sec}^{-1}$ at level 1, $1.7 \times 10^{-6} \text{ sec}^{-1}$ at level 2 and $3 \times 10^{-6} \text{ sec}^{-1}$ at level 3.

D. INTEGRATION SCHEME AND INITIAL CONDITIONS

The time integration is comprised of continuous sections of 1 Matsuno step and 4 leapfrog steps, with a time increment of 6 minutes. The model was initially set to a state of no motion with observed July mean temperature (T^*). The diabatic heating is operative at the end of each integration section (30 minutes).

The model is integrated for 32 days with the results of the last 15 days analyzed and discussed. All resultant fields are interpolated to 3 constant pressure surfaces equal to 250 mb, 500 mb and 850 mb.

III. RESULTS

The principal features of the northern summer monsoon are, in general, quite reasonably simulated by the model. In the following discussion the model results are compared with observations, mainly those by Krishnamurti (1967).

A. TIME MEAN FIELD

The 15-day time mean fields of wind, geopotential height, temperature and vertical velocity are shown in Figs. 4-7. In Fig. 4a the 250 mb wind field shows an anticyclonic center near 31°N , 51°E which resembles the upper-tropospheric Tibetan high although the calculated position is shifted about 30° towards the west. A secondary anticyclonic center situated at 30°N and 20°E resembles that of the Arabian high. The anticyclonic area near 30°N extends eastward to about 130°E . This elongated anticyclonic belt resembles the observed seasonal-mean pattern along 30°N . The belt ends in the Pacific TUTT which as calculated is near $165\text{-}180^{\circ}\text{E}$ and $26\text{-}40^{\circ}\text{N}$, again about 35° to the west of the observed position. The TUTT has a northeast-southwest tilt, but its strength seems to be somewhat weaker than that observed. A "split" trough appears about 24° to the west of the major TUTT. This splitting does not show up in the observed time-mean field, but it has been reported to occur quite frequently on daily maps during summer typhoon seasons (Sadler, 1974). The westward shift of the major features is somewhat expected as has been discussed in the introduction. The underdevelopment of the TUTT is perhaps due to the fact that our heating function is derived

from the 0 - 180°E domain while the observed TUTT is generally to the east of 180°, thus its forcing function cannot be well represented in our model. The southern hemispheric flow pattern does not quite resemble that observed, although anticyclonic cells near 156°E and 44°E are in the general vicinity of the observed southern high areas. The strong easterly jet in the southern periphery of the Tibetan anticyclone reaches a maximum speed of approximately 25 ms^{-1} near 64°E, slightly less than the 30 ms^{-1} speed observed by Krishnamurti.

The 500 mb flow as shown in Fig. 4b is more chaotic, and there is no good observational data field with which to compare. The 850 mb winds (Fig. 4c) clearly show the low-level cyclonic circulation beneath the upper-level Tibetan anticyclone and the mid-Pacific subtropical ridge. Strong southerly cross-equatorial flow dominates most of the equatorial region. This flow turns to southwesterly north of the equator and resembles the low-level monsoon winds. Westward phase shift of circulation centers also occurs at this level and is consistent with upper-level flow.

Fig. 5a shows the 250 mb geopotential field. The Tibetan high is the most outstanding feature while the mid-Pacific TUTT is fairly weak in strength, similar to that indicated by the wind field. At the 850 mb level (Fig. 5c) a deep low area is under the upper high with a small low to the east. A weak ridge is found near the 250 mb TUTT region.

The 250 mb temperature field (Fig. 6a) shows that the Tibetan high is a warm high with warm temperatures extending over the entire high pressure area. The coldness of the TUTT region is also clearly indicated. Similar patterns also appear at 500 mb (Fig. 6b) and 850 mb (Fig. 6c).

Since the heating function includes the upper-level thermal effect of the Tibetan highland, the calculated temperature distribution at the lower levels is probably not too meaningful.

The vertical velocity field at 400 mb as shown in Fig. 7 resembles closely the distribution of the diabatic heating function which is quite expected. Upward motion prevails in the Tibetan warm high area while downward motion prevails in the cold TUTT. A thermal direct circulation which converts planetary-scale potential energy to kinetic energy obviously maintains this circulation. The maximum upward velocity is about -3.5 mb hr^{-1} , or about 2.5 cm s^{-1} .

Figs. 8 and 9 show the mean divergence and vorticity fields, respectively. The 250 mb divergence (Fig. 8a) is a reasonable reproduction of Krishnamurti's observed 200 mb divergence. This indicates that our specified heating function is properly chosen for simulating the forcing. The divergence fields at the 500 and 850 mb levels are direct results of the specified heating and again may be quite different from the real atmosphere. The low-level convergence has an almost opposite pattern as compared to the upper level. Near areas with large 250 mb divergence, strong convergence always occurs at 850 mb and the 500 mb level usually remains weakly convergent. Thus the non-divergent level is between 500 mb and 250 mb which indicates a quite realistic vertical profile. The vorticity fields are representative of the wind fields shown in Figs. 4. The pattern at 250 mb shown in Fig. 9a is very similar to the 200 mb pattern observed by Krishnamurti (1967). The field is dominated by a negative vorticity belt between 8°N and 35°N . The TUTT region is only very slightly indicated by weak positive vorticity north of 25°N near 180°E . A westward phase shift is also evident.

B. TRANSIENT FIELD

Figures 10 and 11 are the time-longitude sections of vorticity and divergence at 12°N and 24°N, respectively, and are constructed in order to study the transient features. The vertical axis is time beginning from hour 444 (day 18) and ending at hour 780 (day 32), in 12 hour segments. The horizontal axis is longitude from 0° to 180°E in 4° increments. The longitudinally averaged zonal velocity changes are also plotted.

Synoptic-scale transient disturbances are very evident at 250 mb but totally absent at the 850 mb level. At 500 mb only near the TUTT region is there some activity. At 12°N the 250 mb vorticity section indicates a zonal wavelength range of 30°-60° with an average of approximately 45°. The averaged phase speed is approximately $10^{\circ} \text{ day}^{-1}$ although it varies somewhat between longitudes. Based on these estimates a periodicity of approximately 5 days is implied. The phase speed is generally lower than the mean zonal wind speeds which range from -14.7 to -16.7 m sec^{-1} .

The transient synoptic-scale wave activities at 250 mb have a significant longitudinal variation. This suggests that localized barotropic instability may be a dominant mechanism. The disturbances seem to develop near longitudes where zonal velocity is large. They will then grow to maximum amplitudes just downstream of the velocity maxima, similar to that found by Colton (1973). There is some indication that the disturbances are less active at the time of strong zonally averaged zonal wind. This may be another indication of barotropic energy processes.

Synoptic-scale disturbances at the 200 mb level have been observed near the Indian easterly jet by Krishnamurti (1971). They have also been observed in the TUTT region by many meteorologists (Sadler, 1967 and others). These disturbances are sometimes observed to develop downward to mid and lower tropospheric levels. It is interesting that we found synoptic-scale transient activities near the TUTT region at the 500 mb level.

At 24°N the synoptic activity is not nearly so prevalent in the vorticity pattern. This may be expected with a weaker zonal flow nearly half that at 12°N. At both latitudes the divergence is not as organized as the vorticity although some transient features are evident at 250 mb.

Examples of wind fields at 250 mb are given in Fig. 12 for a 6 day sequence. The basic planetary-scale features, the easterly jet, the Tibetan high, and the TUTT are similar to those of the time mean features. A positive vorticity center about 10°N and 16°E moves at a speed of slightly more than 8° in 24 hours to a position near 8°E at time 624. The western edge of the same cell may be observed near 180° longitude at the same time. Two days later at time 672, the center is at 178°E longitude. Hence in 3 days the low moved 28° for a phase speed of $9.3^{\circ} \text{ day}^{-1}$ which agrees quite favorably with earlier estimates.

IV. CONCLUSIONS

Since observed 200 mb divergence data was used for forcing, ideally the produced mean 250 mb divergence field should be a near replica of this forcing. This is quite difficult due to the finite differences, imposed boundary conditions, and complicated thermodynamics and dynamics operating in the model. In view of these factors the results obtained from our model may be considered quite reasonable, and one can conclude that the model performance is satisfactory.

As has been found by many previous investigators our model confirms that the upper-level planetary-scale features of the monsoon circulation are mainly a direct response to the mean heating. The westward phase-shift problem also occurs in this model. The model shows that the phase shift at low level is closely related to the upper level.

By establishing the capabilities of the model in simulating the gross features of monsoon by the specified heating, we are in a position to further refine the model to study the monsoon. Specifically, the following experiments may be performed:

1. Expand the domain to cover the entire global area.
2. Increase grid point resolution and number of vertical levels.
3. Incorporate topography.
4. Incorporate a time-dependent component of the specified heating.
5. Incorporate parameterized heating.

These steps should enable us to examine the phase shifting problem, the effect of mountains, and the development of synoptic-scale disturbances and their dynamic and thermodynamic interactions with the larger scales.

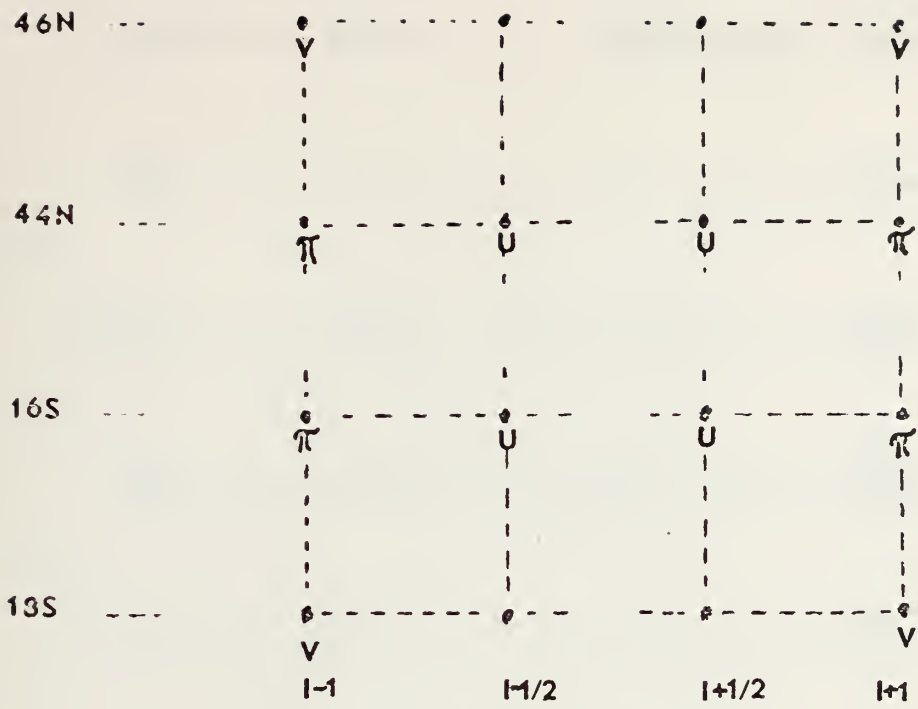


Figure 1. The horizontal distribution of dependent variables. The variables T , Φ , and π are carried at " π -points."

VARIABLE	SIGMA	LEVEL	PRESSURE
$\pi\dot{\sigma}$	0	TROPOPAUSE	100 mb
$V\dot{I}\dot{\Phi}$	1/6	1	250mb
$\pi\dot{\sigma}$	1/3		400mb
$V\dot{I}\dot{\Phi}$	1/2	2	550mb
$\pi\dot{\sigma}$	2/3		700mb
$V\dot{I}\dot{\Phi}$	5/6	3	850mb
$\pi\dot{\sigma}$	1		1000mb

Figure 2. Vertical levels: Sigma is the vertical coordinate. V is the horizontal vector velocity. π is the terrain pressure; T is the temperature and Φ is the geopotential.

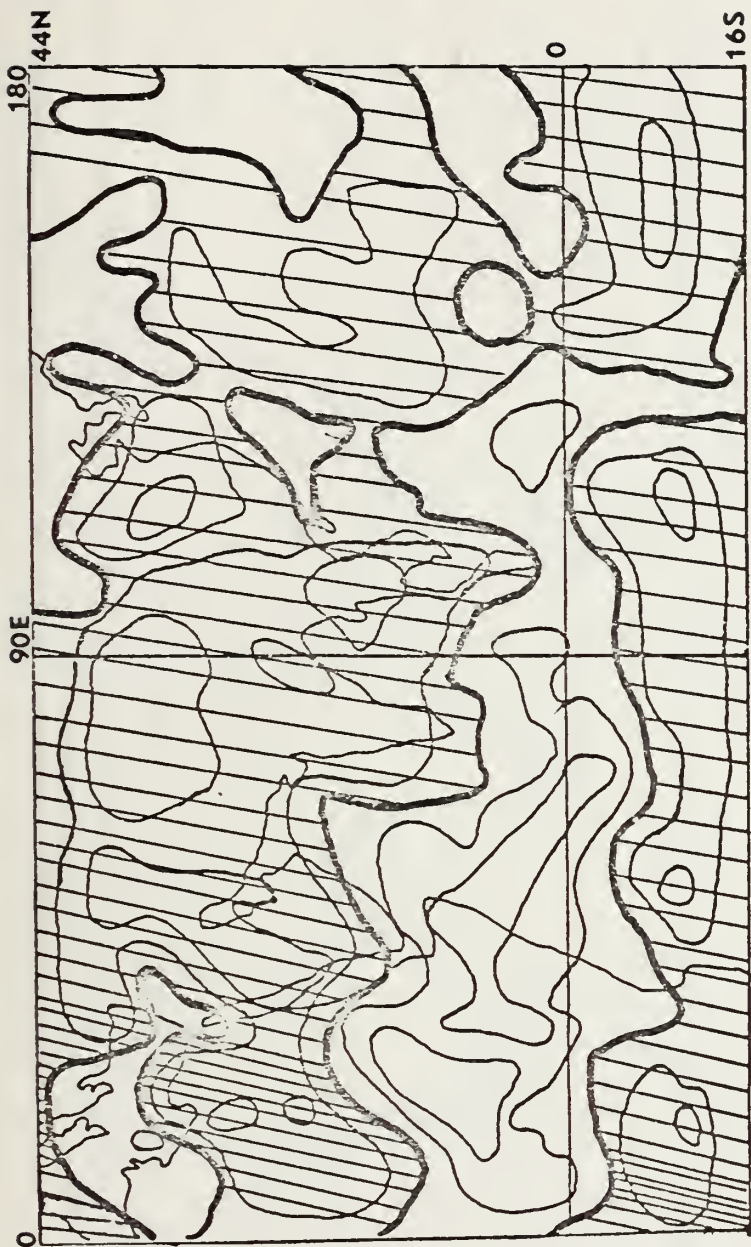


Figure 3. Horizontal distribution of heating. Hatched area indicates positive heating. The interval is $1^{\circ}\text{K day}^{-1}$.

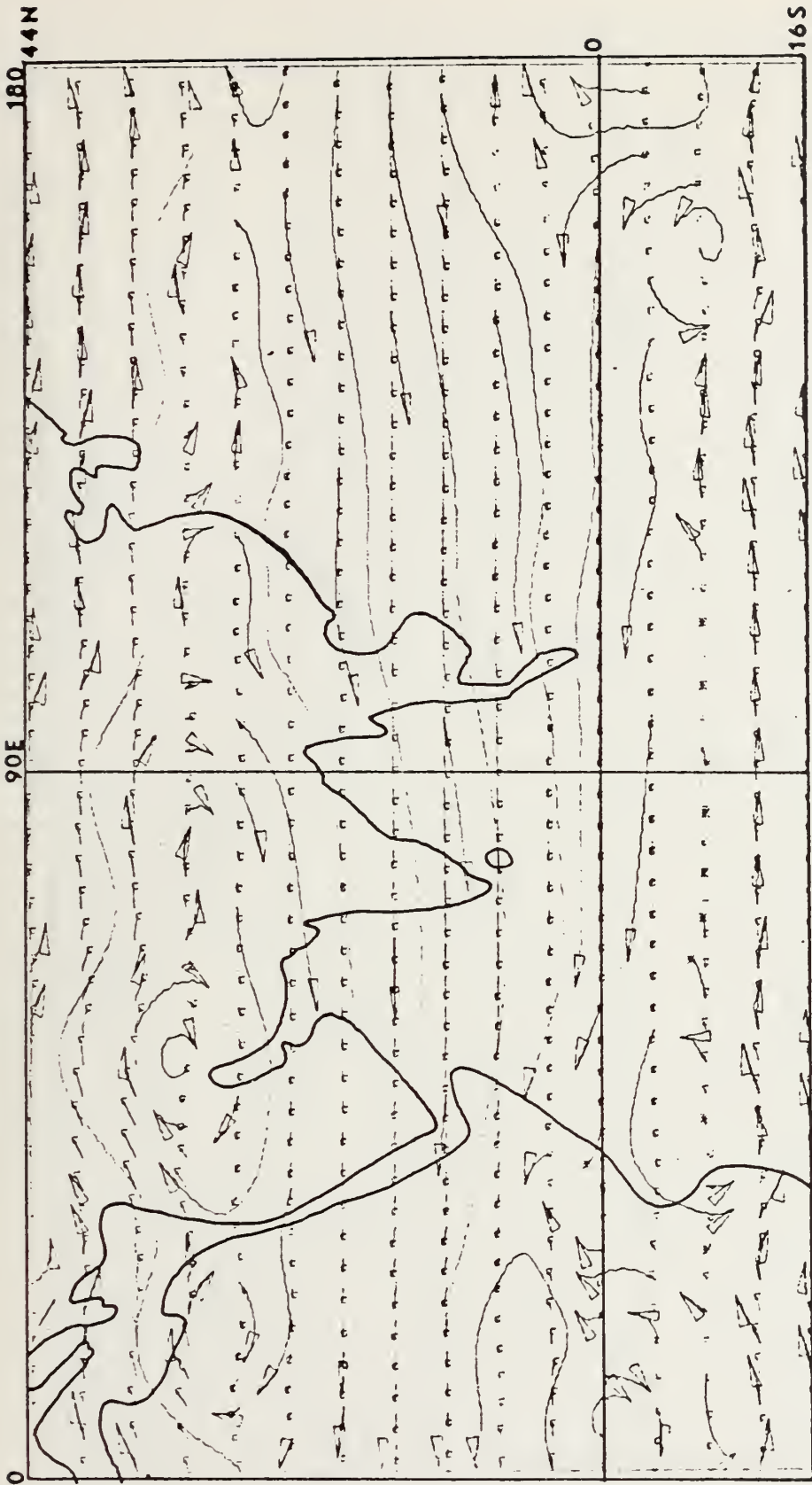


Fig. 4a. 250 mb time-mean wind field.

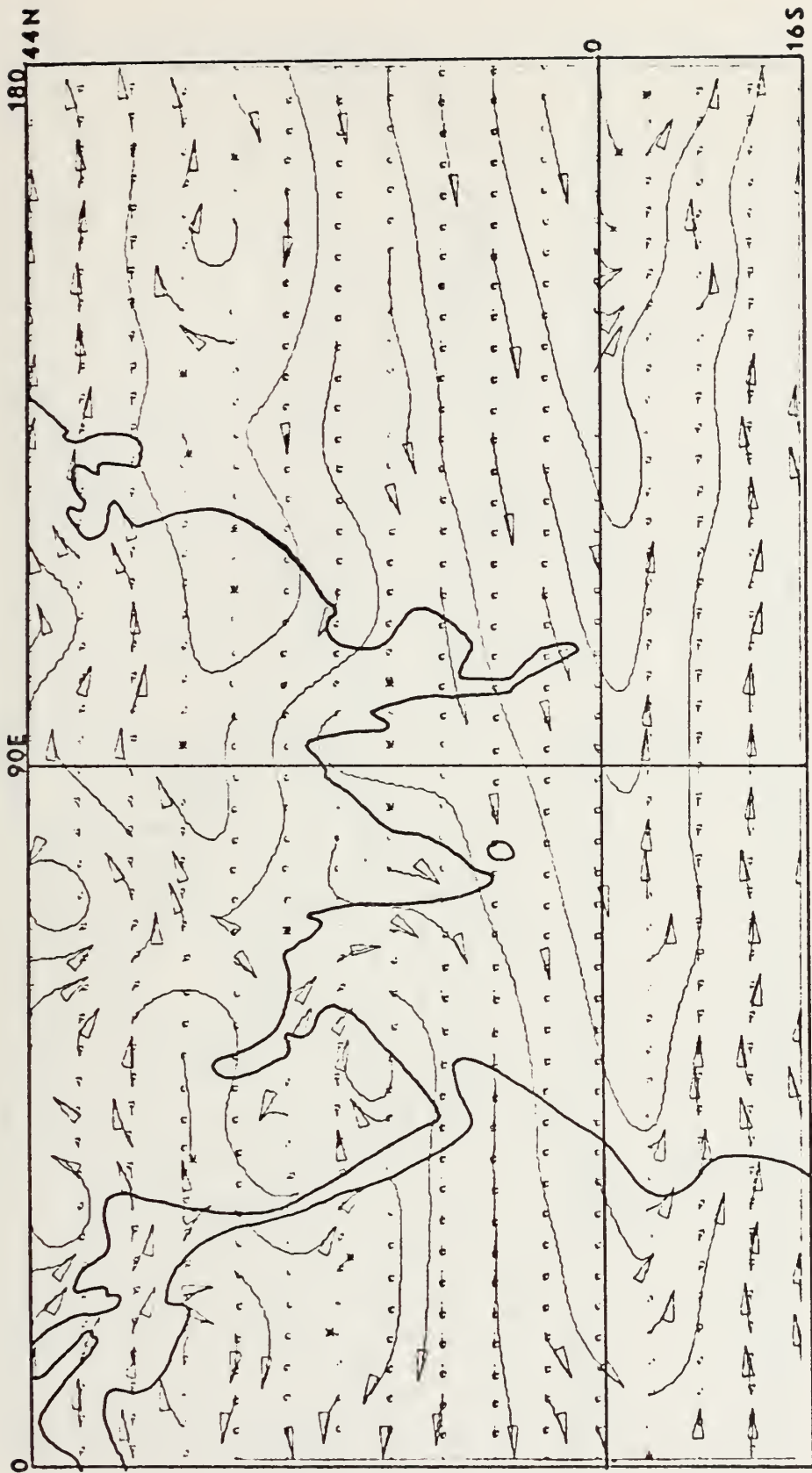


Figure 4b. 500 mb time-mean wind field.

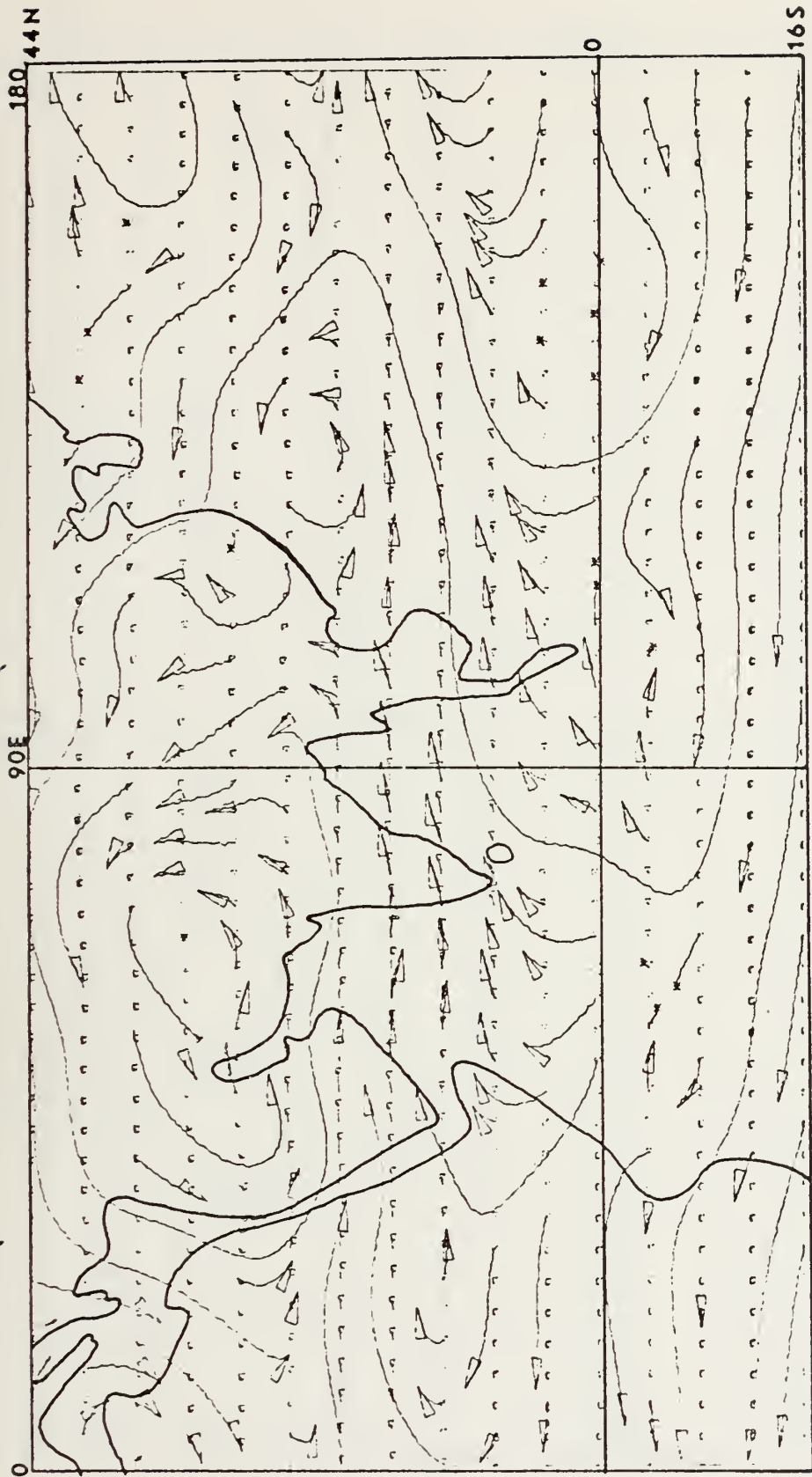


Figure 4c. 850 mb time-mean wind field.

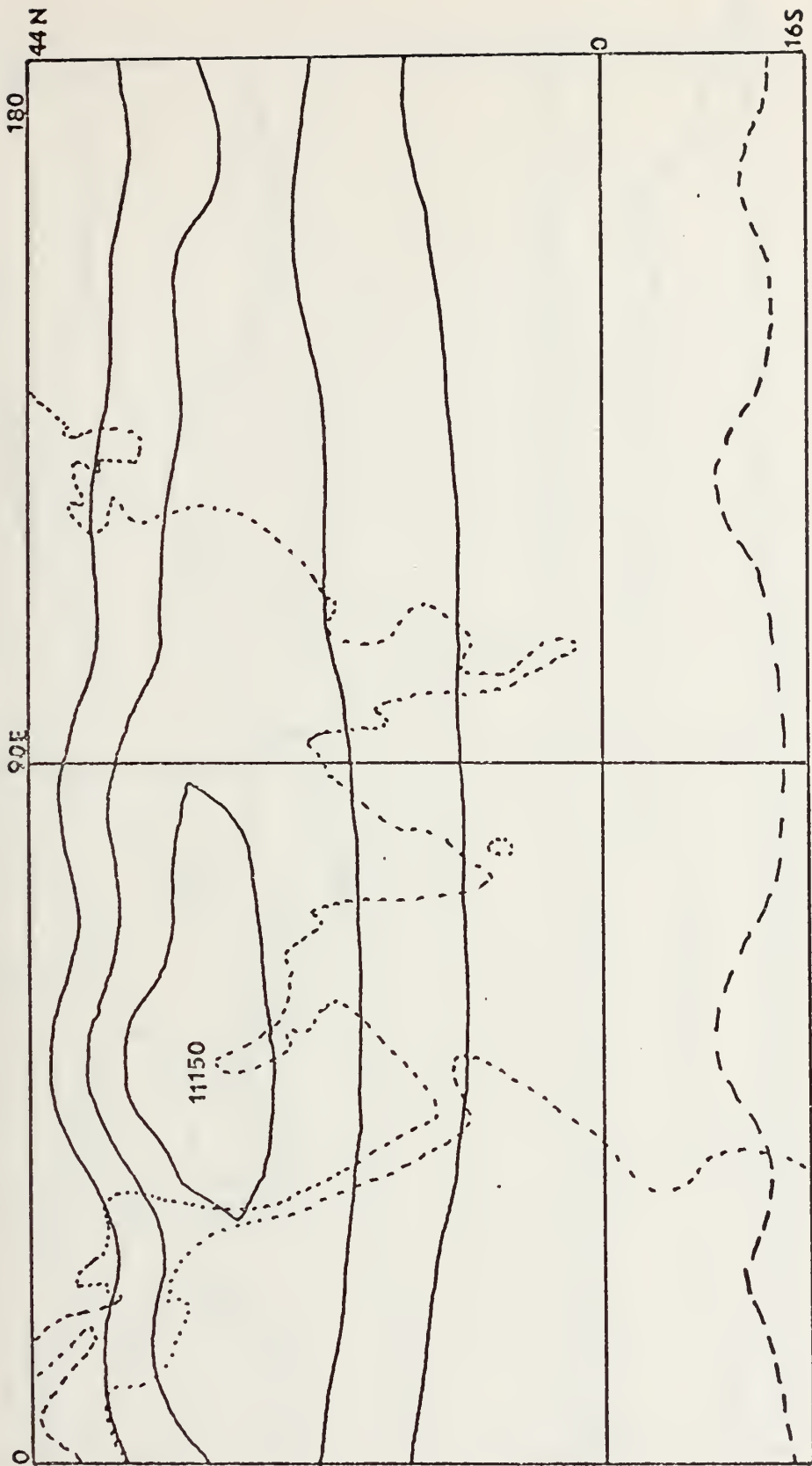


Figure 5a. 250 mb time-mean geopotential field. Interval is $50 \text{ m}^2 \text{ s}^{-2}$.

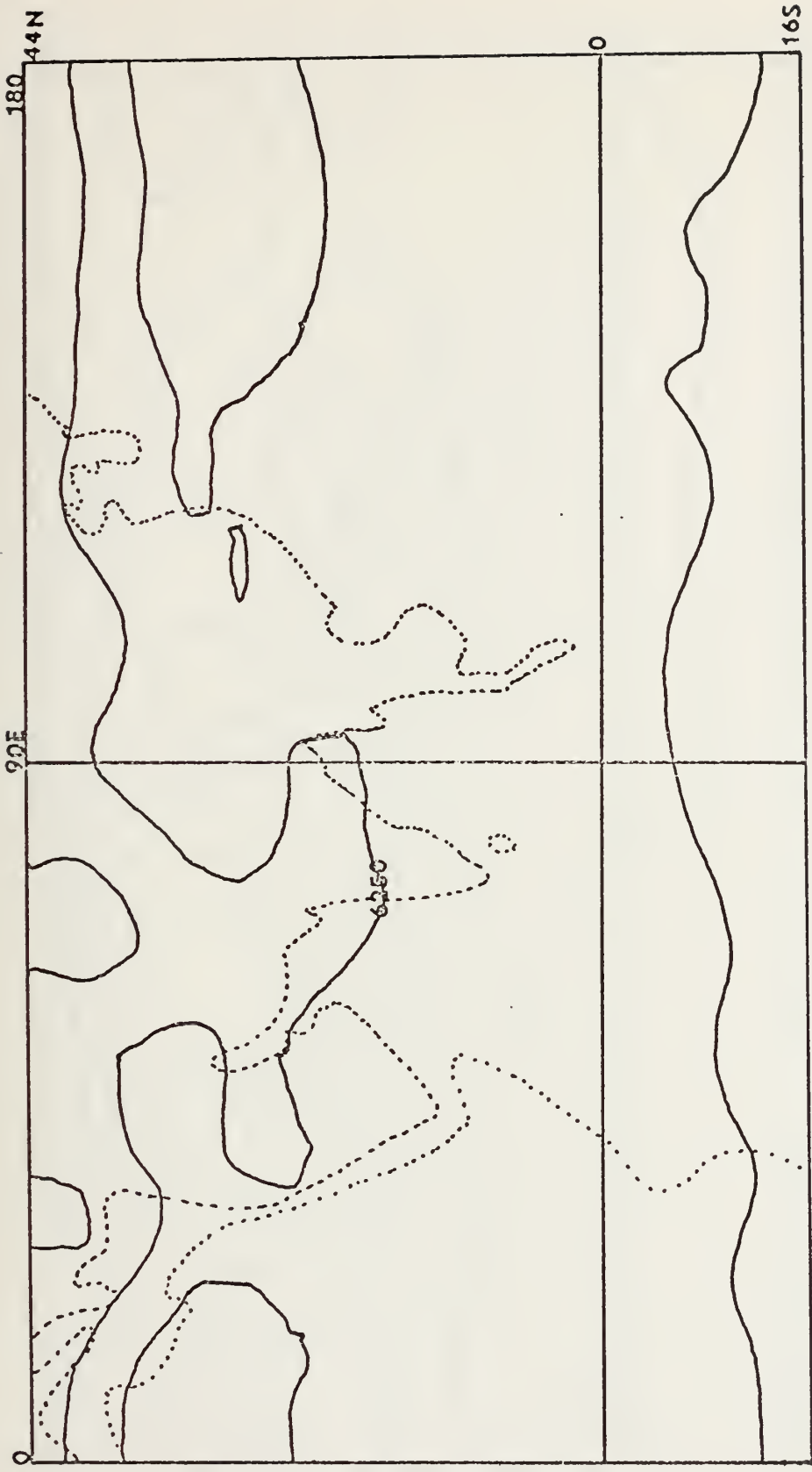


Figure 5b. 500 mb time-mean geopotential field. Interval is $25 \text{ m}^2 \text{ s}^{-2}$.

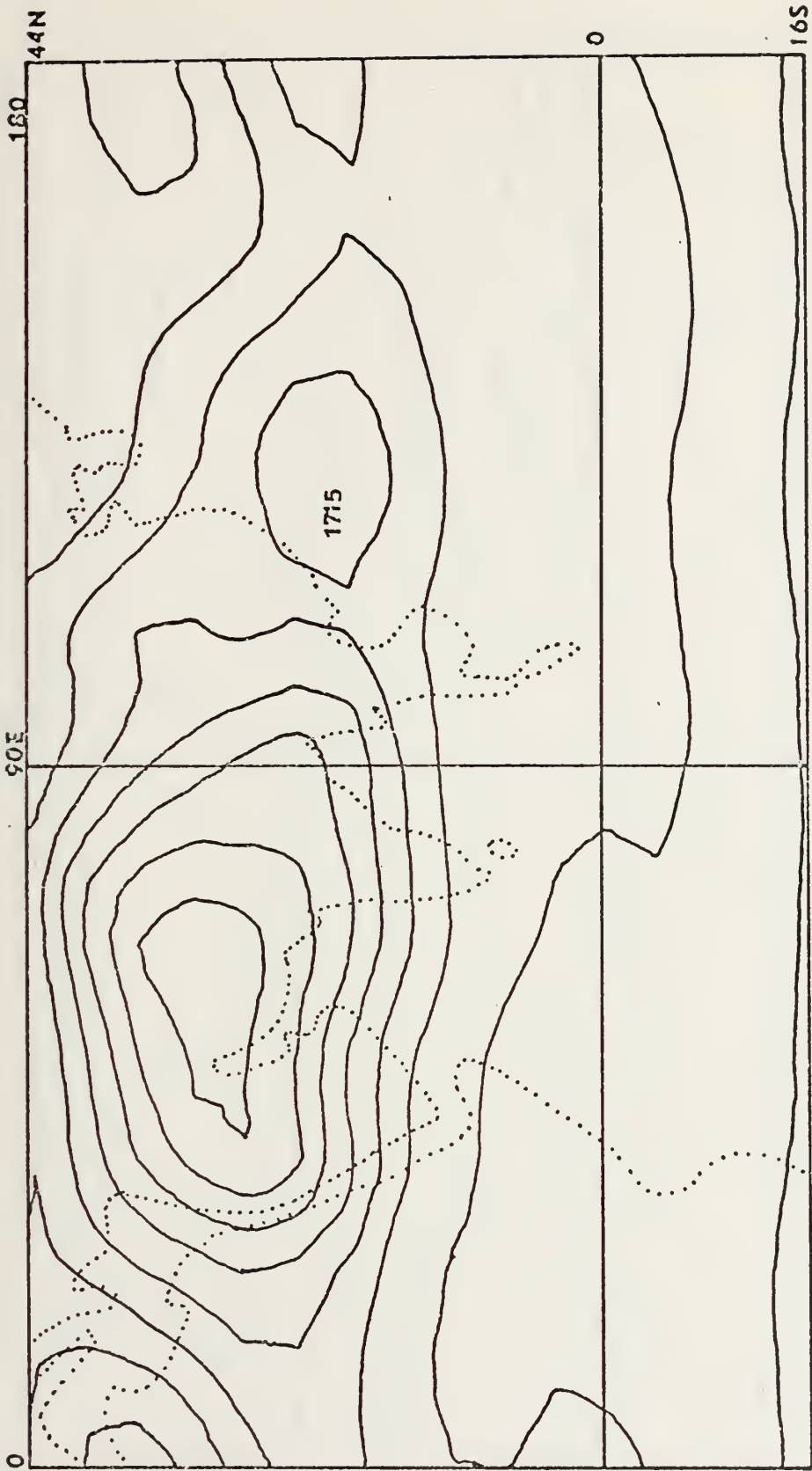


Figure 5c. 850 mb time-mean geopotential field. Interval is 15 m² s⁻².

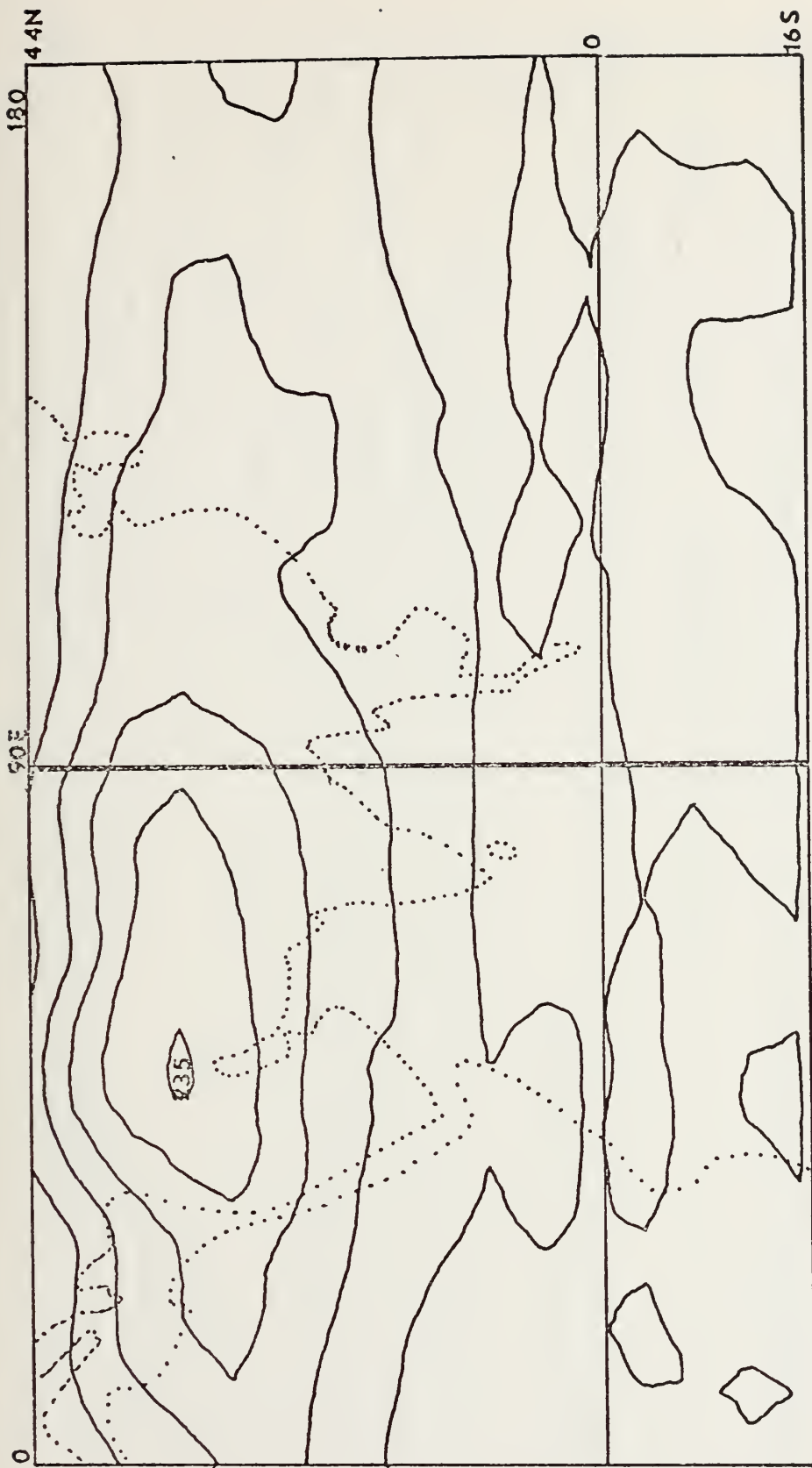


Figure 6a. 250 mb time-mean temperature field. Interval is 1°K.

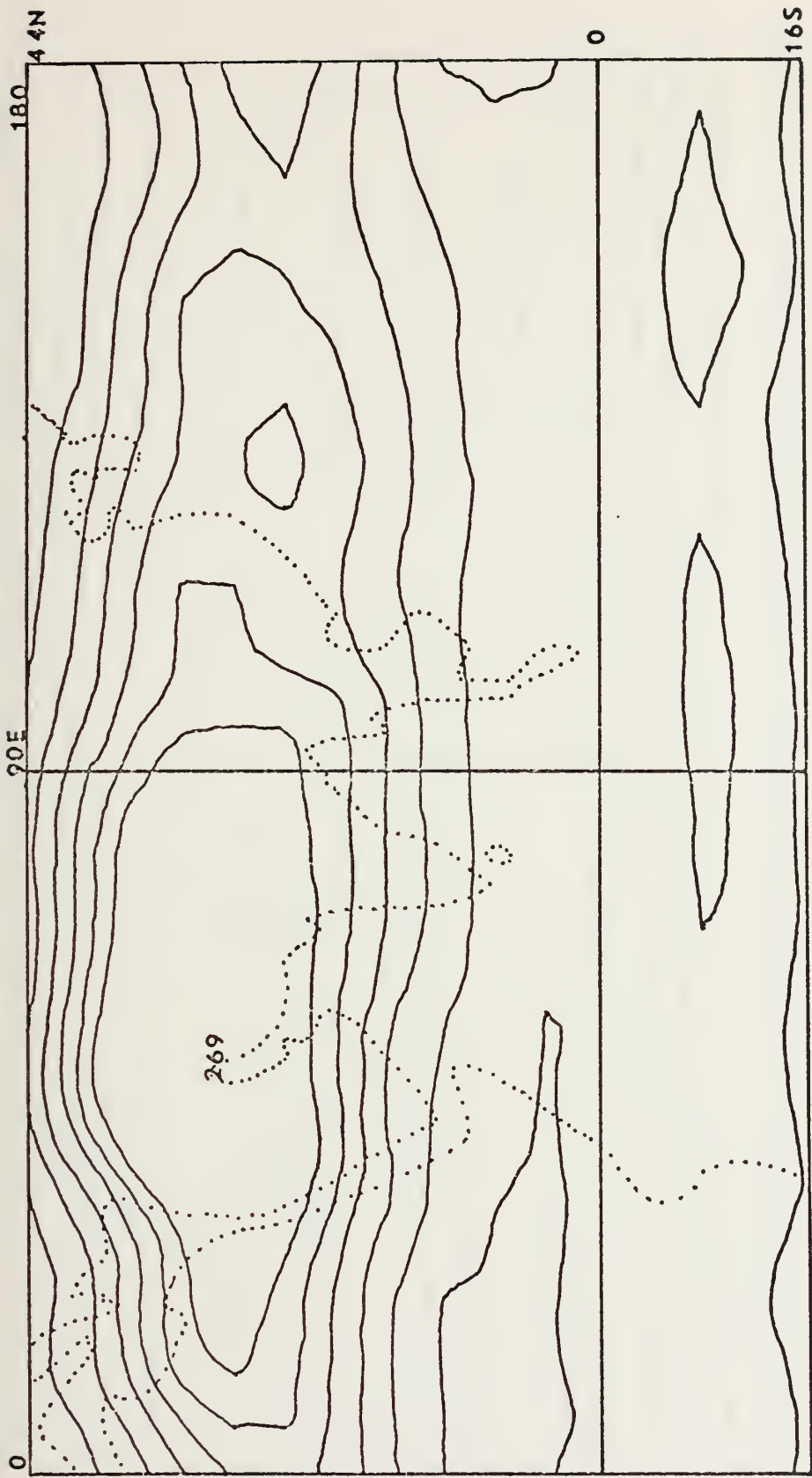


Figure 6b. 500 mb time-mean temperature field. Interval is 1°K.

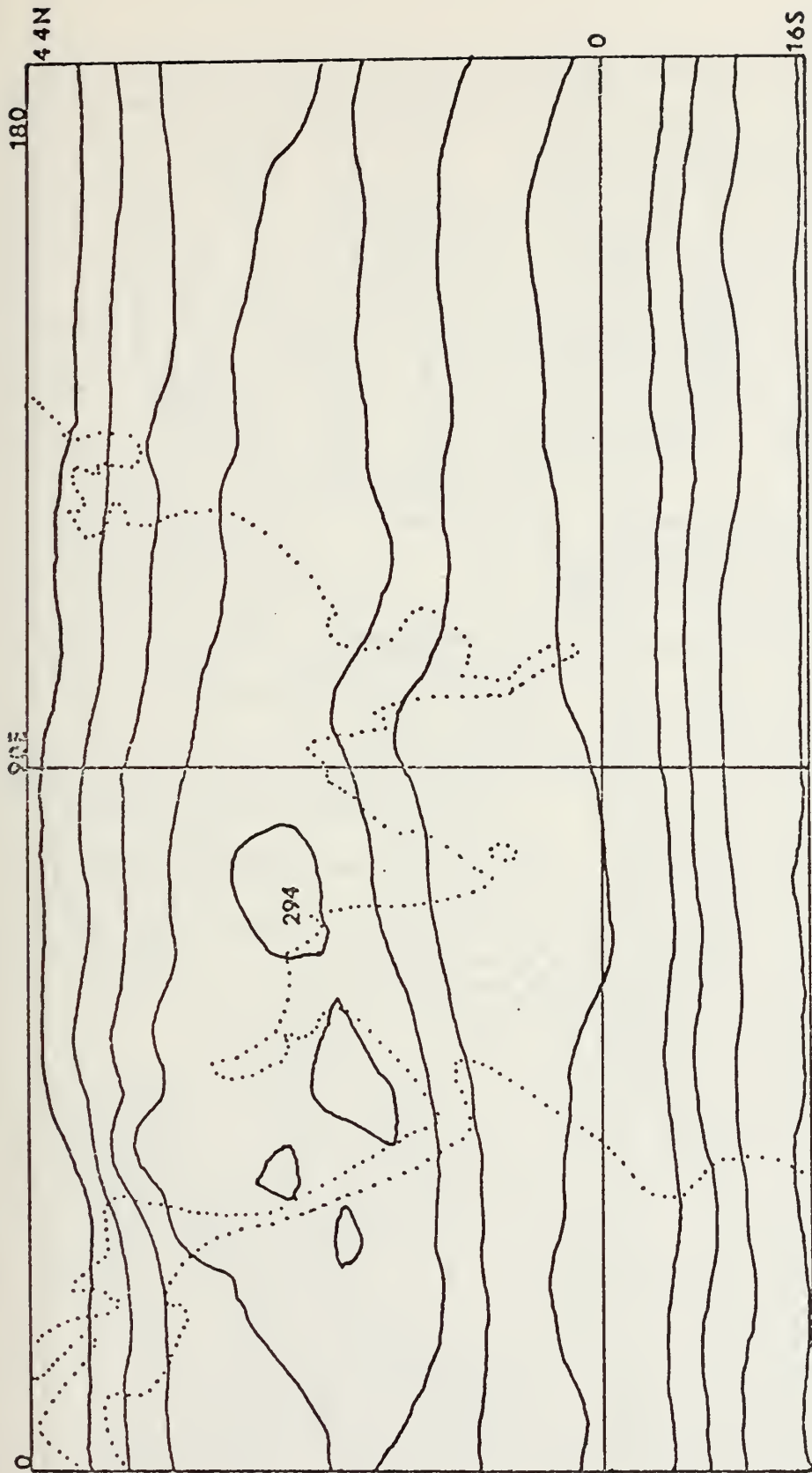


Figure 6c. 850 mb time-mean temperature field. Interval is 1°K.

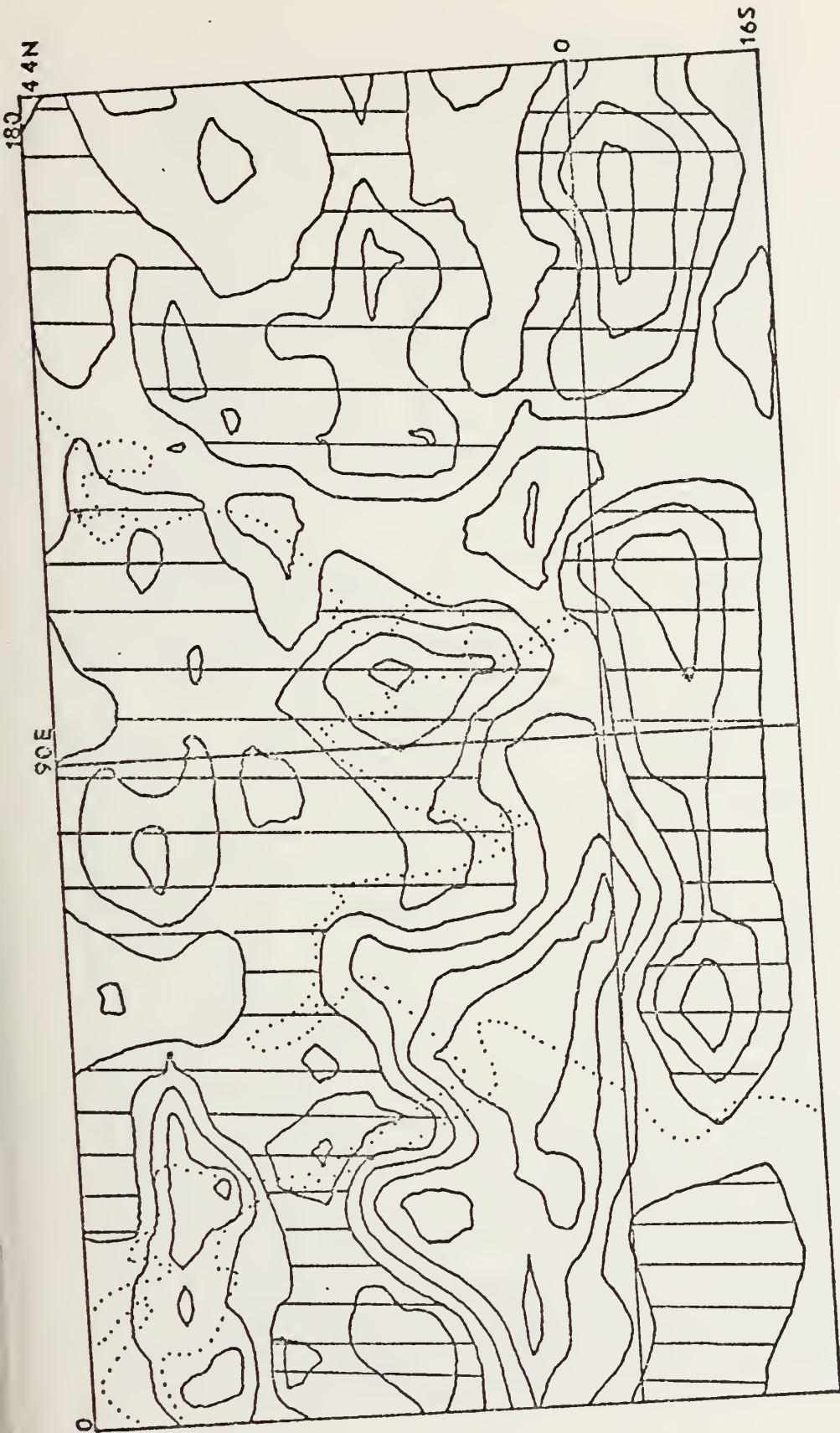


Figure 7. 400 mb time-mean vertical velocity. Cross hatching indicates negative values. Interval is 1 mb hr^{-1} .

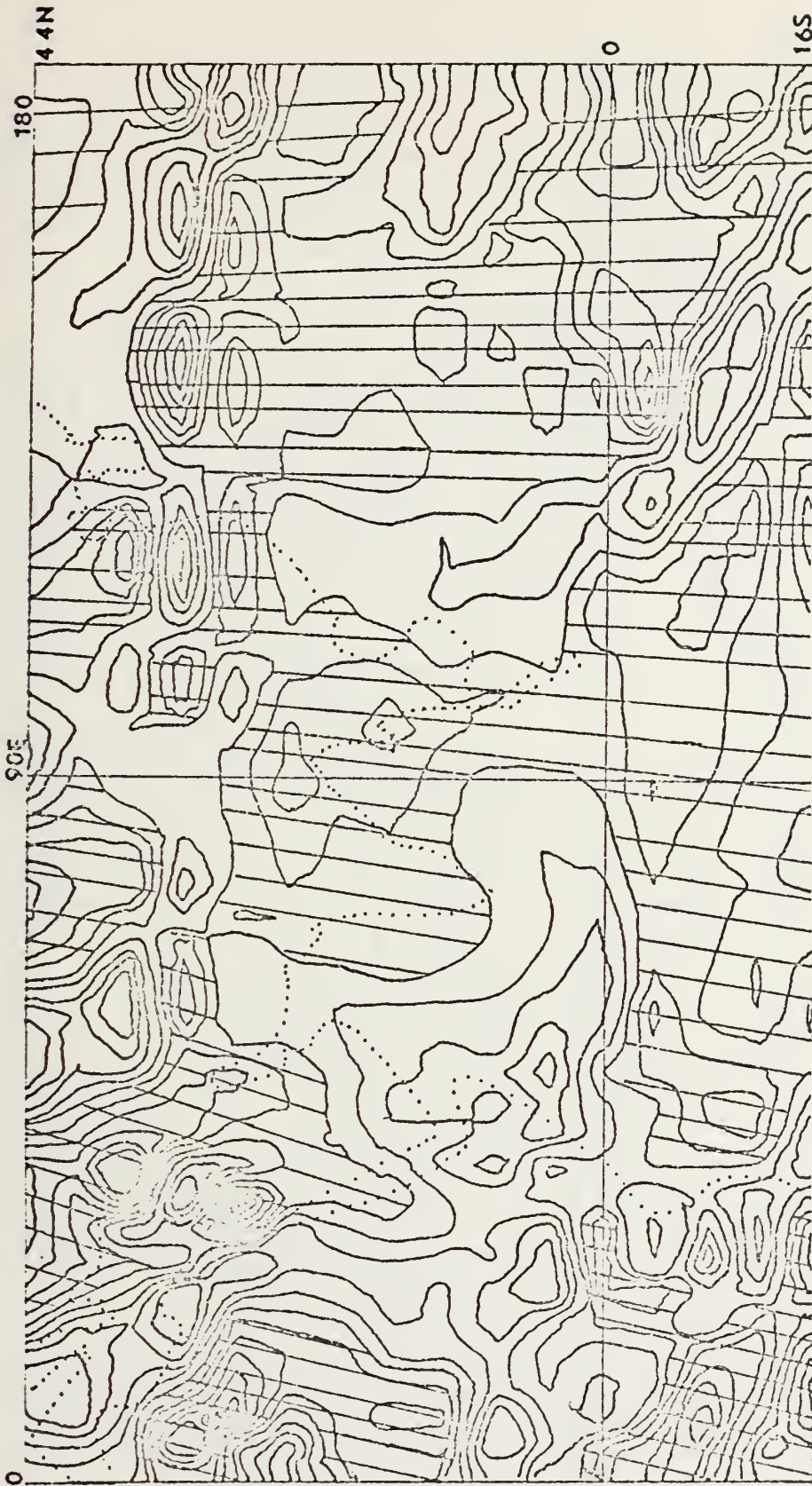


Figure 8a. 250 mb divergence. Cross hatching indicates positive values. Interval is 10^{-6} s^{-1} .

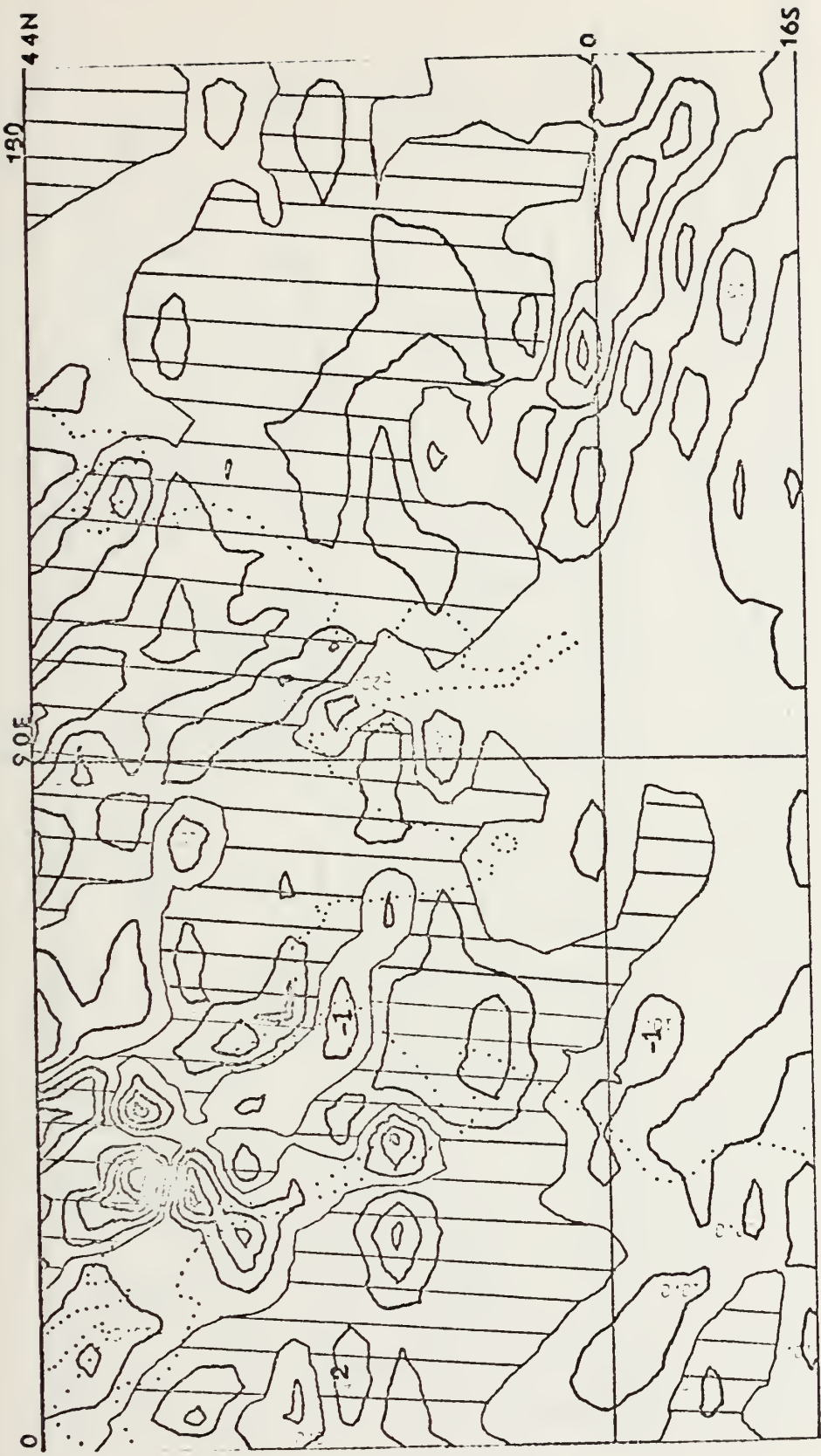


Figure 8b. 500 mb divergence. Cross hatching indicates positive values. Interval is 10^{-6} s^{-1} .



Figure 9a. 250 mb time-mean vorticity field. Interval is 10^{-5} sec^{-1} .

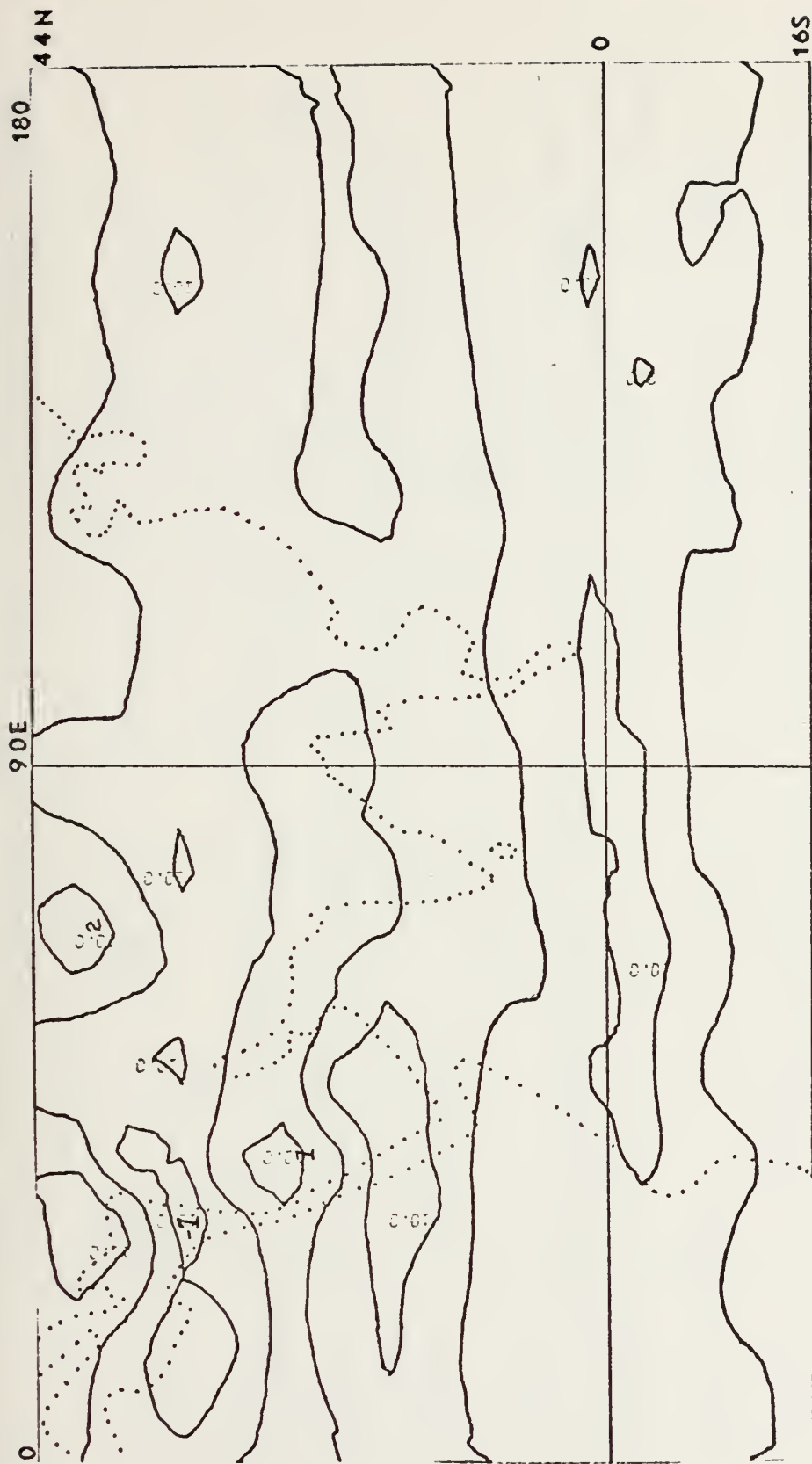


Figure 9b. 500 mb time-mean vorticity field. Interval is 10^{-5} s^{-1} .



Figure 9c. 850 mb time-mean vorticity field. Interval is 10^{-5} s^{-1} .

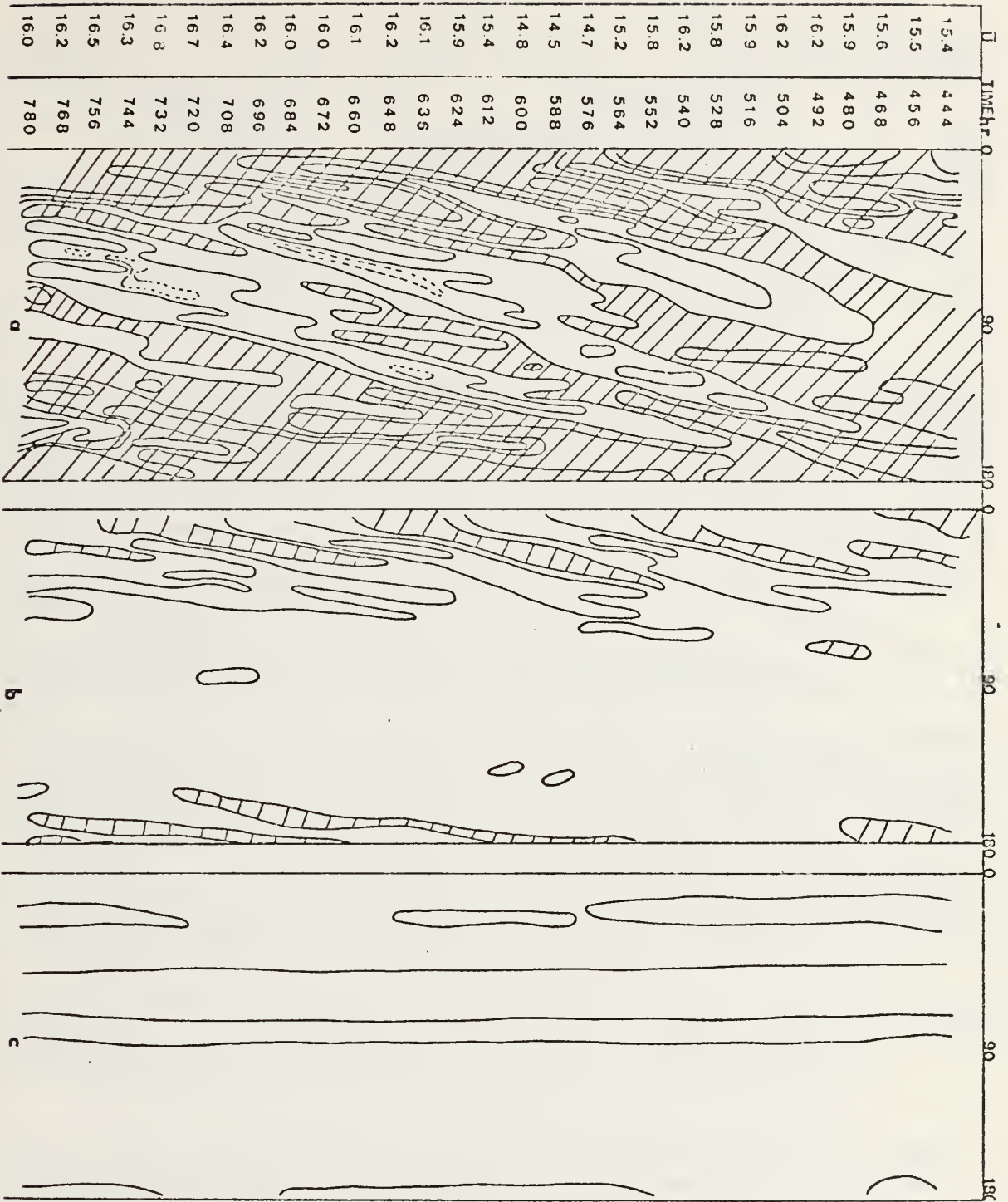


Figure 10a. Time-longitude section of vorticity at 12°N for a. 250mb, b. 500mb, and c. 850mb. The interval is $1 \times 10^{-5} \text{ s}^{-1}$. \bar{u} represents the longitudinally averaged mean zonal wind.

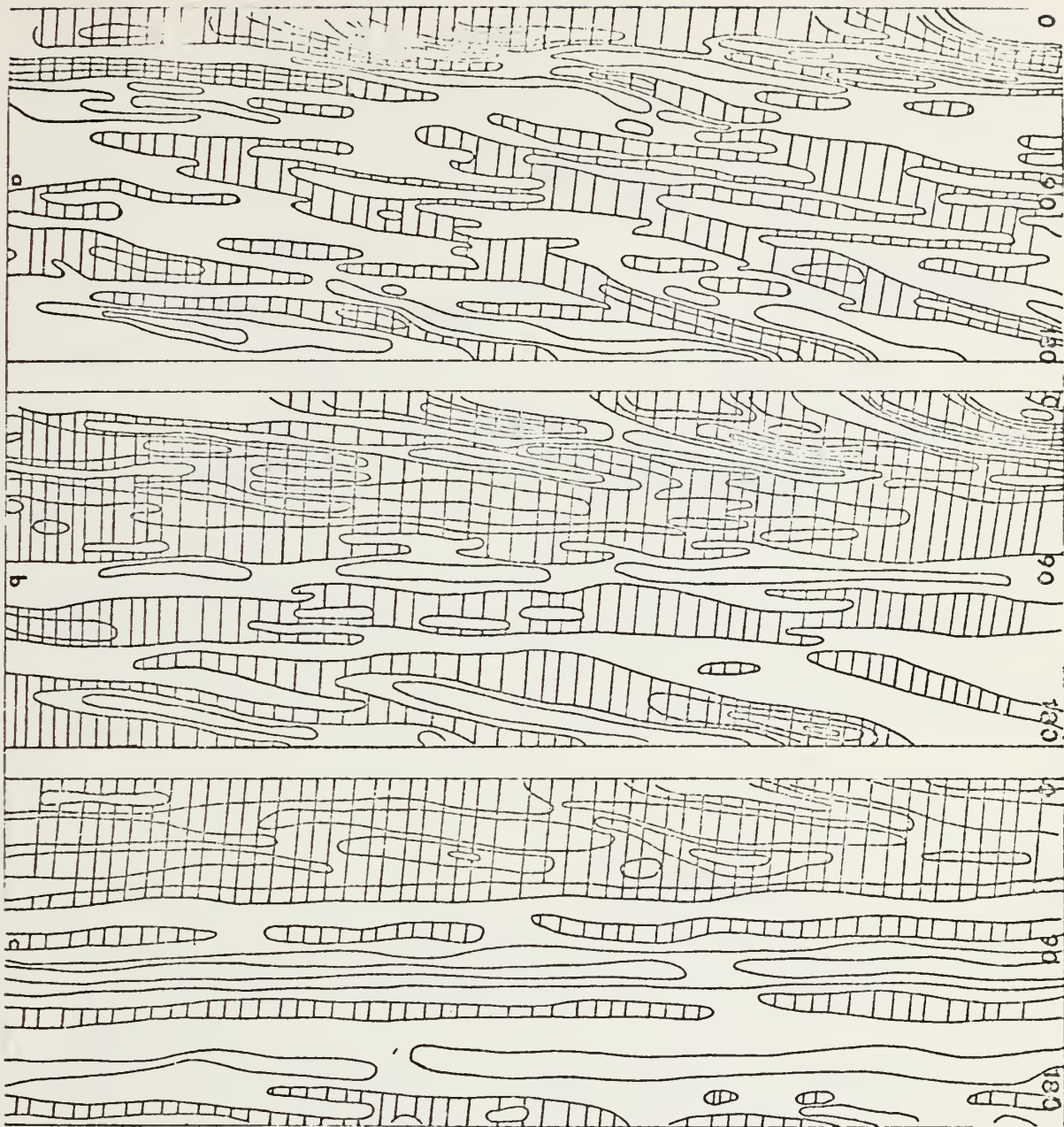


Figure 10b. Time-longitude section of divergence at 12°N for a. 250mb, b. 500mb and c. 850mb. The intervals are $5, 2, \text{ and } 1 \times 10^{-6} \text{ s}^{-1}$, respectively. The time index is shown on preceding vorticity chart.

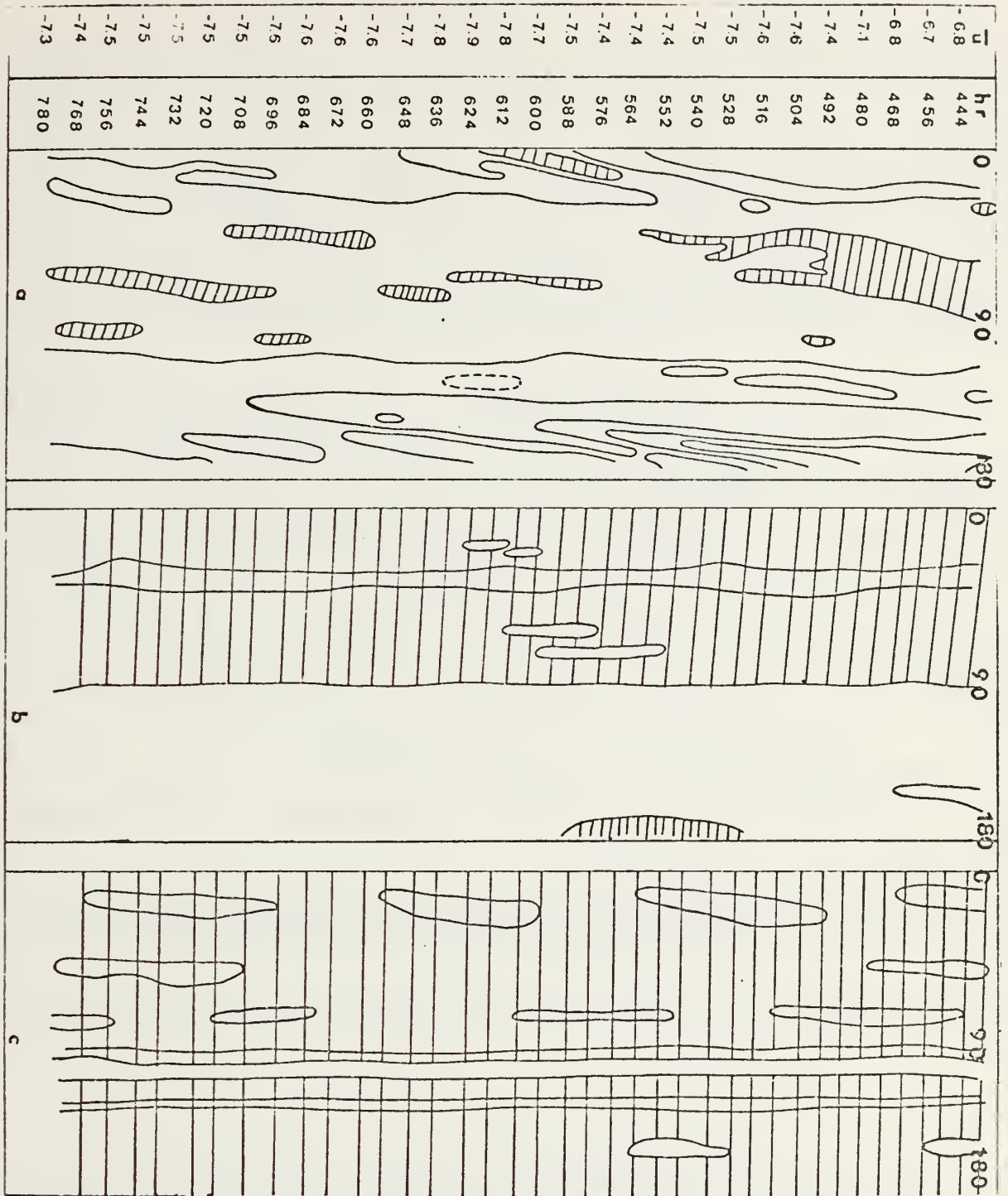


Figure 11a. Time-longitude section of vorticity at 24°N for a. 250mb, b. 500mb and c. 850mb. The interval is $1 \times 10^{-5} \text{ s}^{-1}$. \bar{u} represents the longitudinally averaged mean zonal winds.

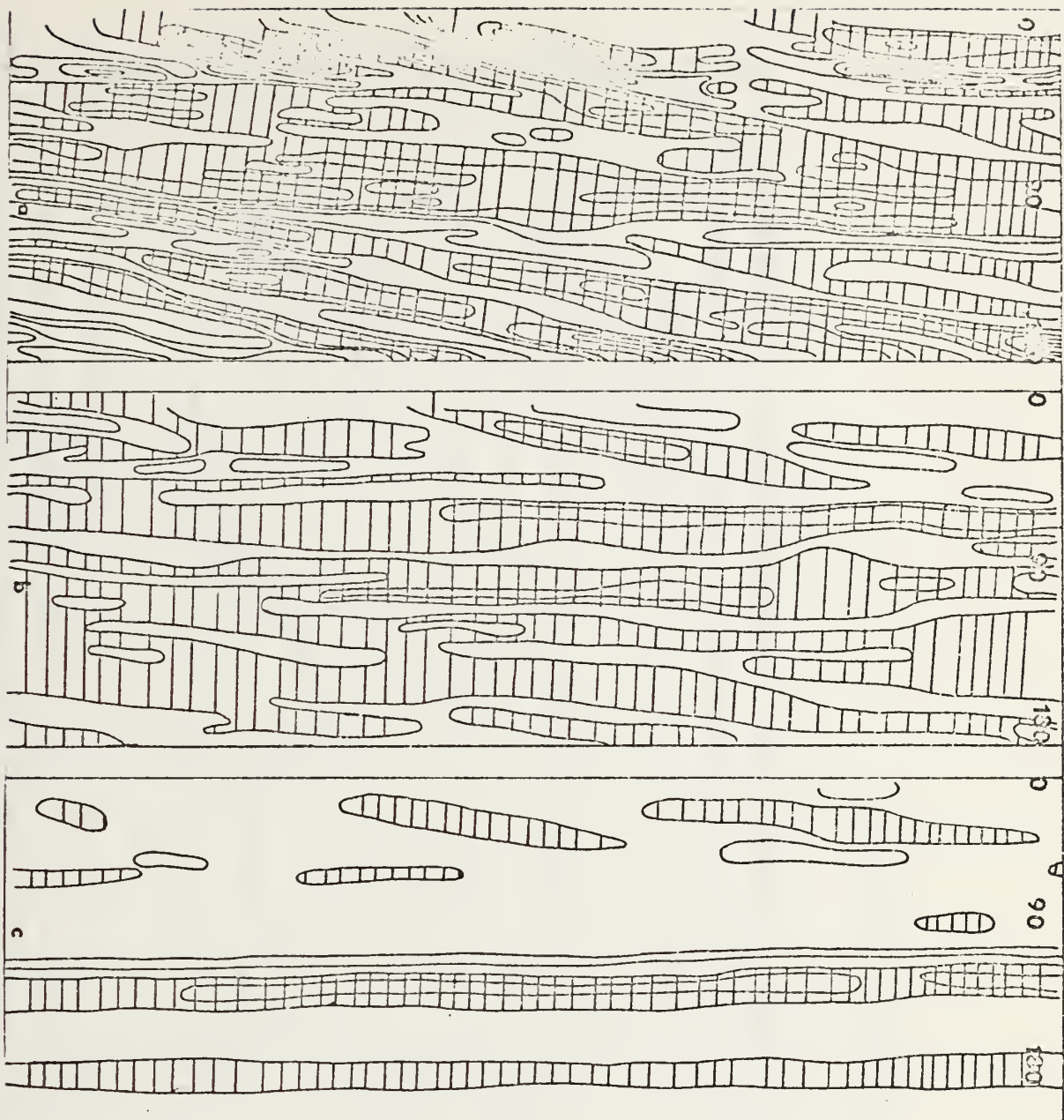


Figure 11b. Time-longitude section of divergence at 24°N is shown for a. 250mb b. 500mb and c. 850mb. The interval is $2 \times 10^{-6} \text{ s}^{-1}$. The time index is shown on preceding vorticity chart.

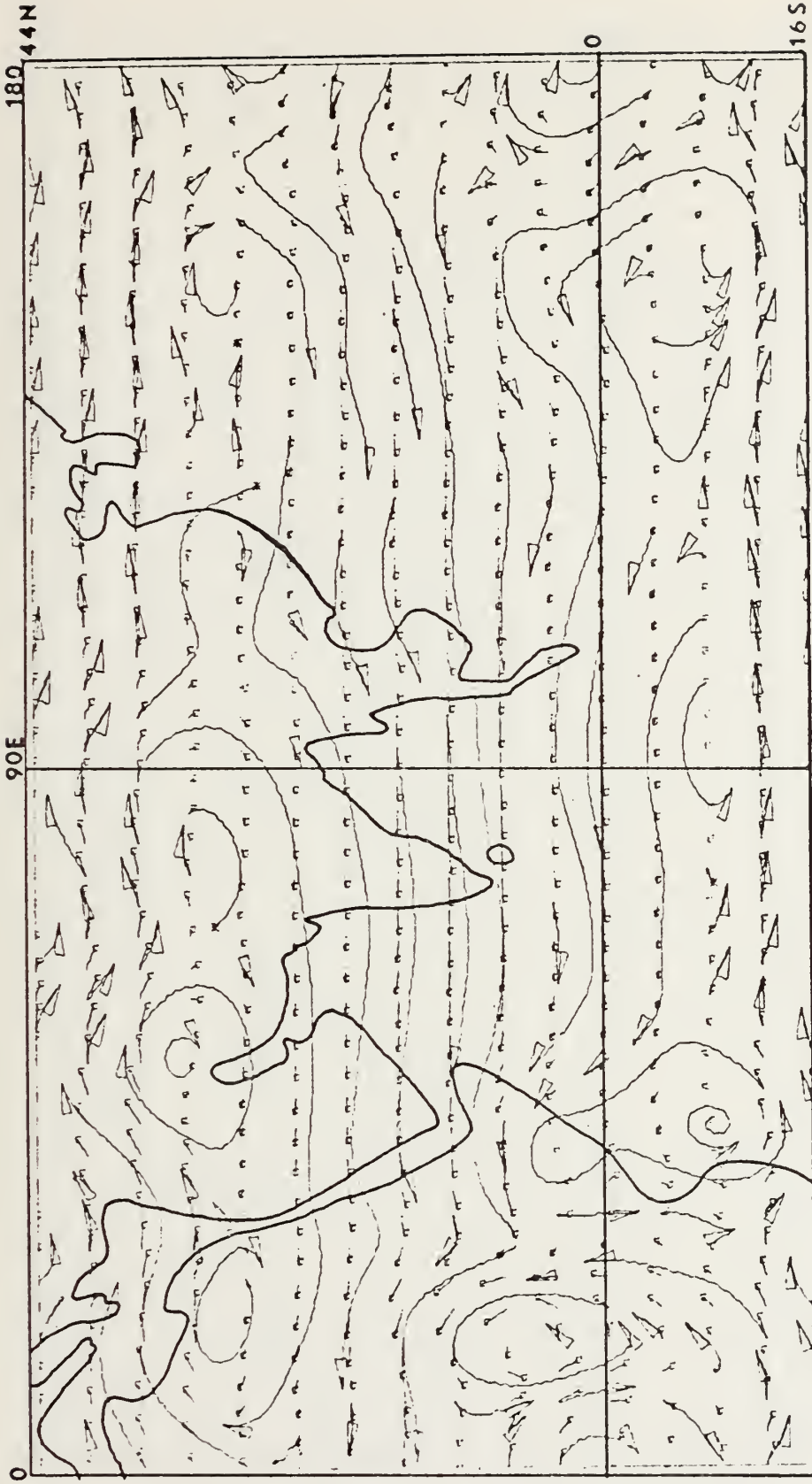


Figure 12a. 250 mb wind field at day 25.

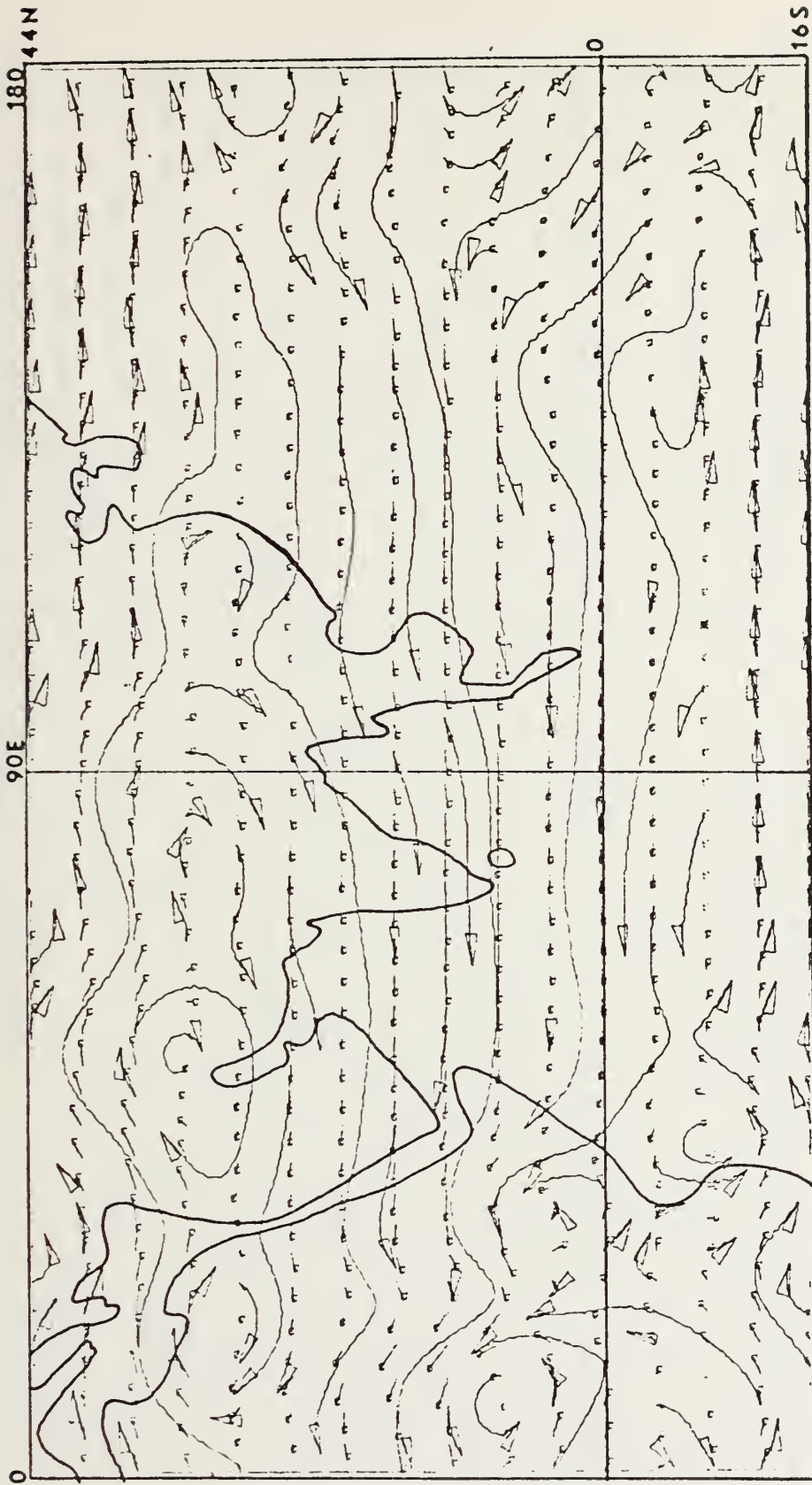


Figure 12b. 250 mb wind field at day 26.

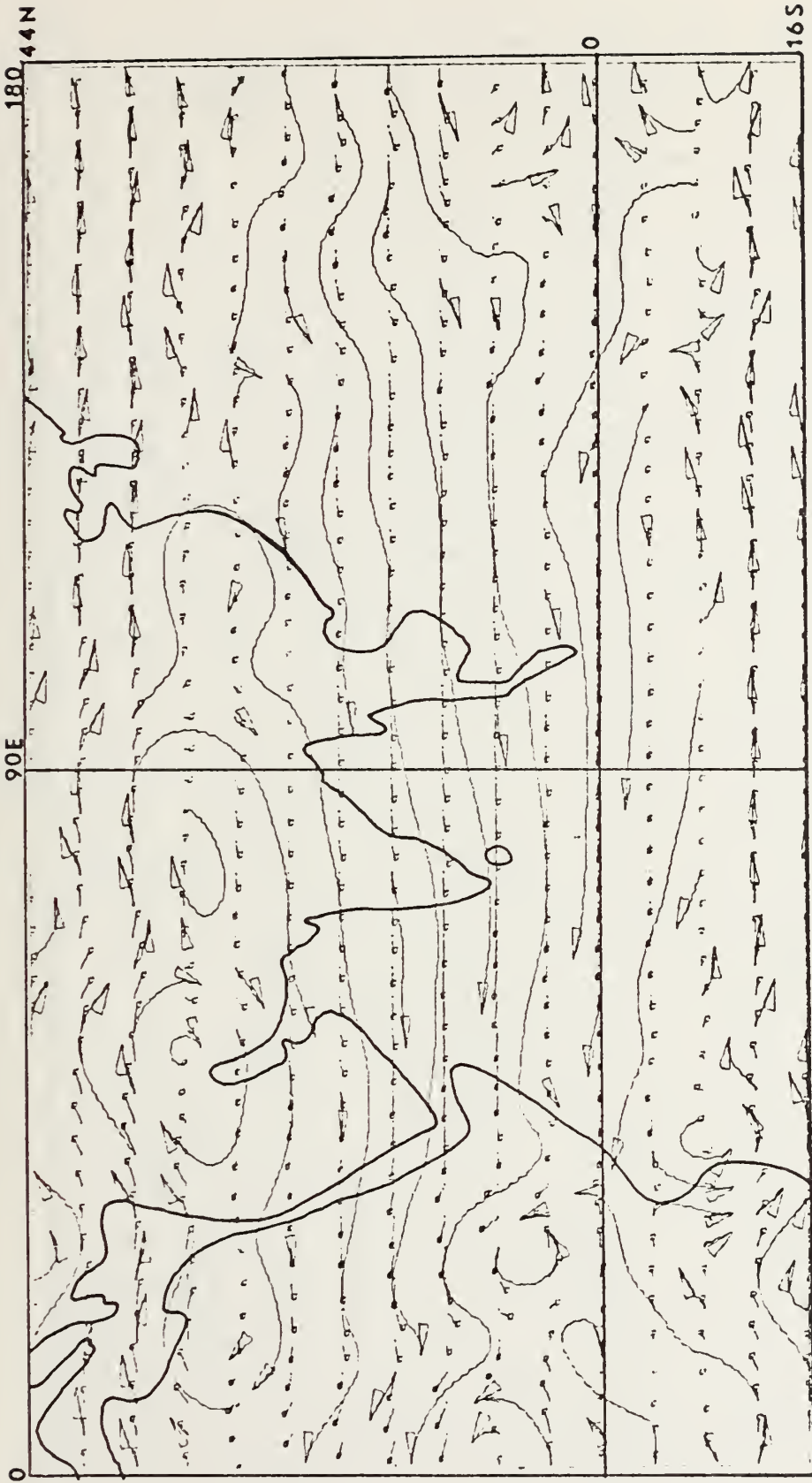


Figure 12c. 250 mb wind field at day 27.

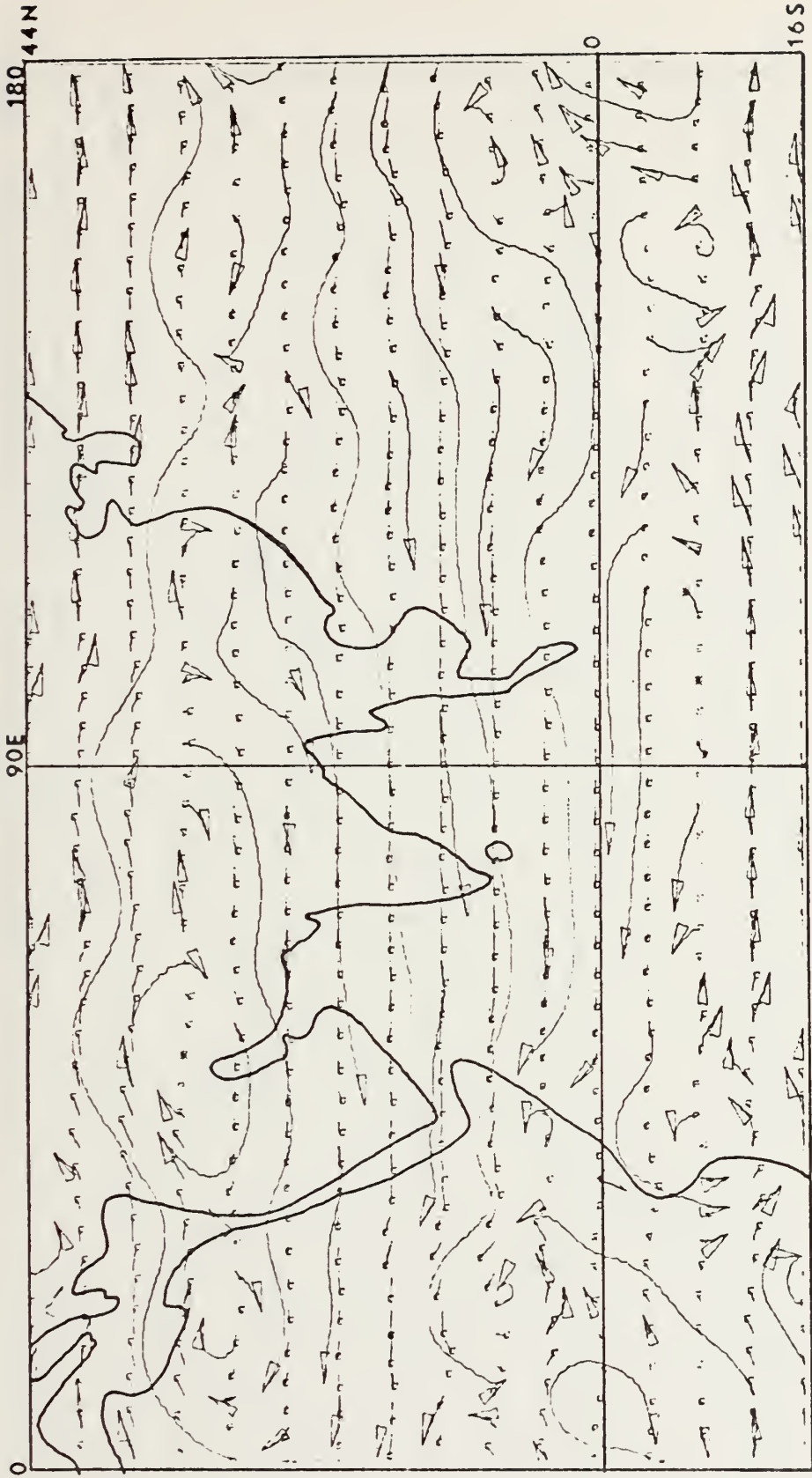


Figure 12d. 250 mb wind field at day 28.

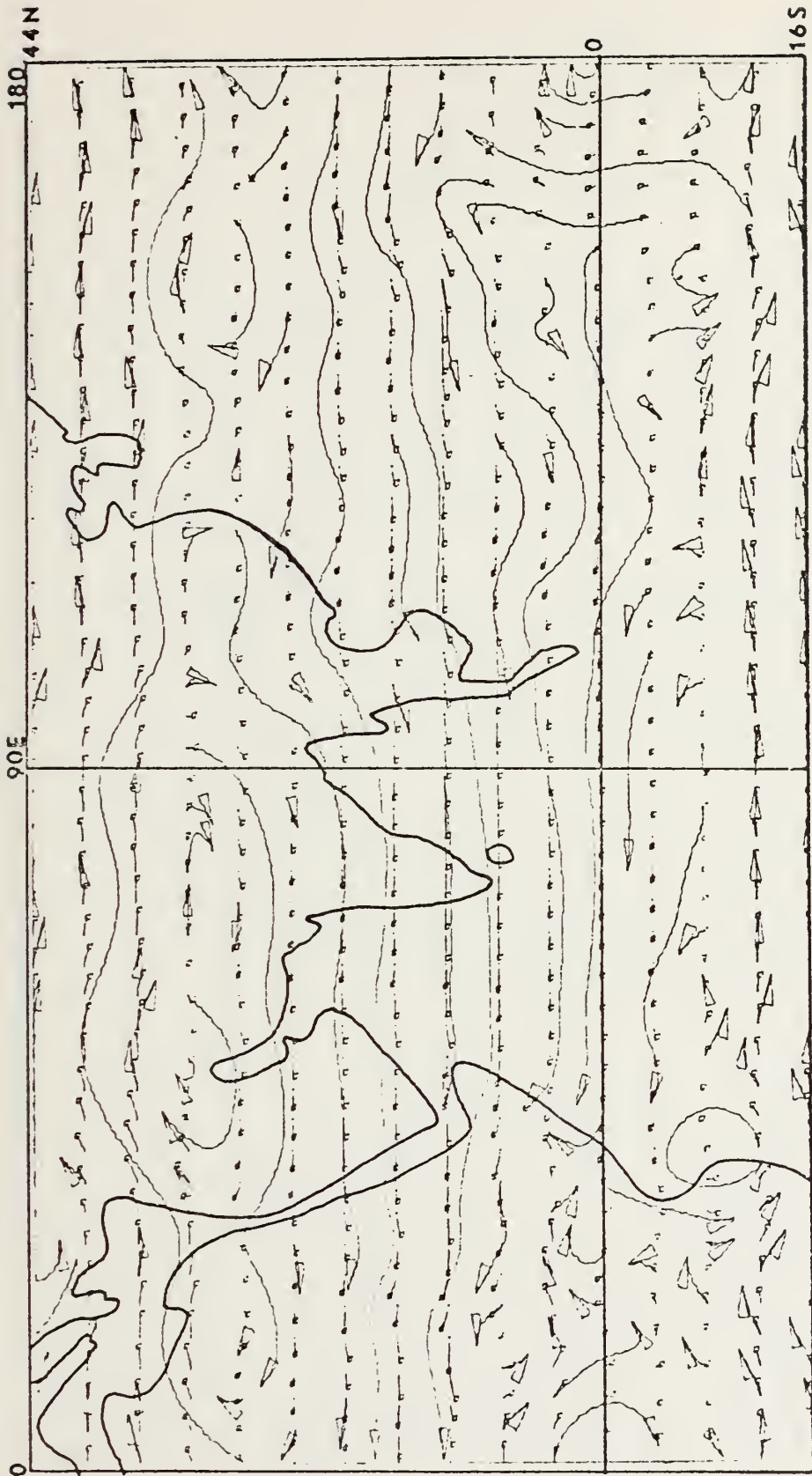


Figure 12e. 250 mb wind field at day 29.

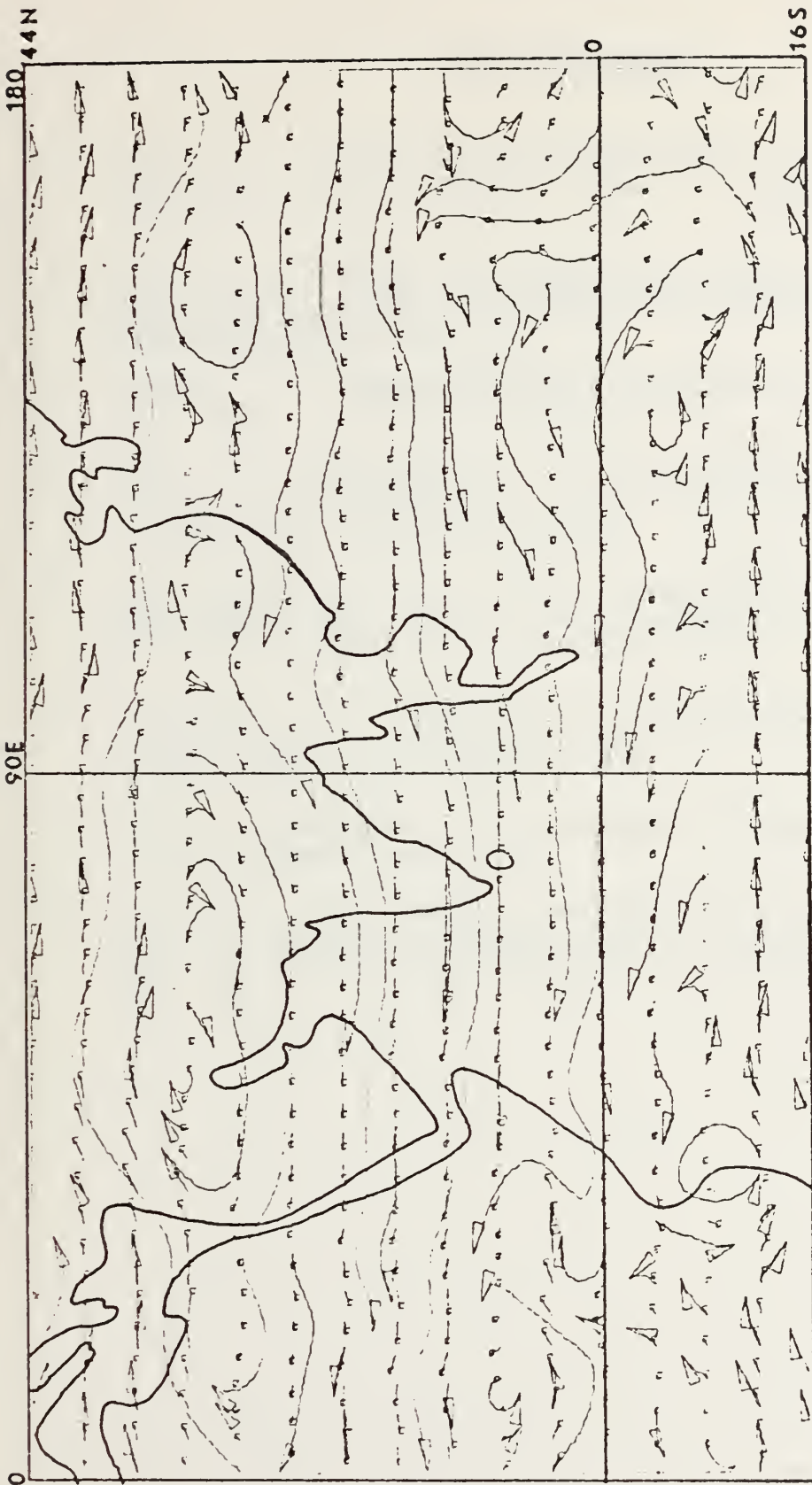


Figure 12f. 250 mb wind field at day 30.

LIST OF REFERENCES

1. Colton, D. E., "Barotropic scale interactions in the tropical upper troposphere during the northern summer." J. Atmos. Sci., 30, 1287-1302, 1973.
2. Gates, W. L., Batten, E. S., Kahle, A. B., and Nelson, A. B., A Documentation of the Mintz-Arakawa Two-Level Atmospheric General Circulation Model, Rand, 1971.
3. Haltiner, G. J., Numerical Weather Prediction, 193-196, 231-238, Wiley, 1971.
4. Holton, J. R., and Colton, D. E., "A diagnostic study of the vorticity balance at 200 mb in the tropics during the northern summer." J. Atmos. Sci., 29, 1124-1128, 1972.
5. Krishnamurti, T. N., and Rogers, B., 200 Millibar Wind Field June, July, August, 1967, Rpt. No. 70-2, Department of Meteorology, Florida State University, Tallahassee, 1970.
6. Krishnamurti, T. N., "Observational study of the tropical upper tropospheric motion field during the Northern Hemisphere summer." J. Appl. Meteor., 10, 1066-1096, 1971.
7. Palmen, E. and Newton, C. W., Atmospheric Circulation Systems, 441-453, Academic Press, 1969.
8. Sadler, J. C., The tropical upper tropospheric trough as a secondary source of typhoons and a primary source of tradewind disturbances. Final Rept., Contract AF19(628)-3860, Air Force Cambridge Research Labs, 1967.

INITIAL DISTRIBUTION LIST

	No. Copies
1. Defense Documentation Center Cameron Station Alexandria, Virginia 22314	2
2. Library (Code 0212) Naval Postgraduate School Monterey, California 93940	2
3. Asst. Prof. C.-P. Chang, Code 51Cj Department of Meteorology Naval Postgraduate School Monterey, California 93940	6
4. Lcdr James R. Bellis VAQ 129 NAS Whidbey Island Oak Harbor, Washington 98277	2
5. Professor George J. Haltiner Chairman, Department of Meteorology Naval Postgraduate School Monterey, California 93940	3
6. Department Library Department of Meteorology Naval Postgraduate School Monterey, California 93940	1
7. Naval Oceanographic Office Library (Code 3330) Washington, D. C. 20373	1
8. Commander, Naval Weather Service Command Naval Weather Service Headquarters Washington Naval Yard Washington, D. C. 20390	1
9. Fleet Numerical Weather Central Naval Postgraduate School Monterey, California 93940	1
10. Environmental Prediction Research Facility Naval Postgraduate School Monterey, California 93940	1

11. Professor J. R. Holton 1
Department of Atmospheric Sciences
University of Washington
Seattle, Washington 98195
12. Dr. Roger T. Williams 1
Department of Meteorology
Naval Postgraduate School
Monterey, California 93940
13. Lt. Anthony V. Monaco 1
NWSED NAF Sigonella
FPO New York 09523

Thesis
B36528
c.1

Bellis

The modelling of
monsoon circulation
during northern summer.

162306

06

er.

Thesis
B36528
c.1

Bellis

The modelling of
monsoon circulation
during northern summer.

162306

thesB36528

The modelling of monsoon circulation dur



3 2768 002 13002 3

DUDLEY KNOX LIBRARY